Waypoint Tracking for Fixed-Wing Unmanned Aircraft Under Multiple Constraints

Haizhao Liang*

School of Aeronautics and Astronautics, Sun Yat-Sen University, Shenzhen, 518106, China

Abstract: This paper investigates the waypoint tracking and the finite-time (FINT) attitude control problems of six-degree-of-freedom fixed-wing unmanned aircraft subject to asymmetric input saturation (AIS), angular velocity constraints, and external disturbances. First, an attitude error that describes the difference between the ballistic frame and the desired frame is defined, such that the flight direction in the inertial frame can be regulated by integrating attitude control method, thereby achieving waypoint tracking. Second, we propose a smooth AIS model to handle the AIS problem and a nonlinear mapping function to address the angular velocity constraints. These approaches yield a constraint-free system and reduce the mixed-constraint problem to ensuring the boundedness of all signals. Then, by using the backstepping method, the robust adaptive control technique, and an introduced FINT disturbance observer, a FINT control law is designed to regulate the actual flight direction of the aircraft. The FINT convergence of the attitude and airspeed tracking errors is guaranteed using the Lyapunov theory. Finally, numerical simulation is conducted to validate the effectiveness of the proposed control law.

Keywords: Asymmetric input saturation, constrained angular velocity, fixed-wing unmanned aircraft, finite-time control, waypoint tracking.

1. INTRODUCTION

Due to the multifunctional capabilities of fixed-wing unmanned aircraft (FW UA), guidance and control problem for UA has been a subject of considerable concern from both the academic and industrial communities in recent decades [1-5]. For underactuated systems, including FW UA, it is extremely challenging in practical scenarios to develop guidance methods that enable them to track designated trajectories. In contrast, waypoint tracking is a more effective guidance scheme that requires fewer computational resources and has significant practical value [6]. By appropriately designating waypoints, different types of underactuated vehicles are able to carry out diverse operational tasks, including object detection, target tracking, and aerial/underwater photography. As a result, waypoint guidance for unmanned systems has attracted considerable research interest; however, only a few waypoint guidance designs exist for FW UA [7-11]. It is noticeable that the outputs of the actuators of a six-dgree-of-freedom (6-DOF) FW UA always encounter magnitude saturation constraints resulted from the limited performance of actuation components [12, 13].

The issue of input magnitude saturation presents widely in numerous practical physical systems [14]. Anti-saturation control approaches for different types of aerospace vehicles such that has received enormous research interests. In [15-20], the saturation functions, hyperbolic tangent functions, and saturation models that are affine in model inputs were employed to capture the input saturation property and hence the input signals can not violate the magnitude restrictions. However, the symmetric input saturation models cannot be directly implemented to describe the asymmetric input saturation (AIS) characteristic. Some works were put forward to counter the AIS constraints using AIS models that are non-affine in the model inputs [16, 21-24], which introduces additional complexity for control design. For FW UA, the AIS constraint generally refers to the amplitude limits applied to the thrust upper bounded by a positive constant depending on engine performance and lower bounded by the idle thrust. Efforts have been made to overcome the AIS constraints applied to the thrust components of UA, using saturation functions [16, 24]. It is noteworthy that actuation components for the rotational subsystem can also facing the AIS problem. For instance, control surfaces can jam at a non-neutral position due to impact, wear, or foreign object debris such that the maximum upward deflection might be decreased. Obviously, the outputs of actuators still cannot follow the designed control input signals under the AIS fault, which leads to severe degradation of control performance. Hence, it is desirable to derive an anti-AIS fault control method for FW UA. However, the AIS constraint applied to the control surfaces of FW UA has been investigated by few literature. Nevertheless, little attention has been paid to the problem of angular velocity constraints [14, 25, 26].

The issue of constrained angular velocity, meaning the amplitude restrictions on rotating rate of the aircraft

*Address correspondence to this author at the School of Aeronautics and Astronautics, Sun Yat-Sen University, Shenzhen, 518106, China;
Email: lianghch5@mail.sysu.edu.cn

body, is also critical for FW UA control [25]. A FW UA may be subject to angular velocity constraint resulting from concerns regarding the structural strength of the fuselage or the particular requisites of the mission [14, 27]. Hence, it is of great significance to deal with the problem of constrained angular velocity. Research efforts have been dedicated to solving the control problem for state-constrained systems in recent years and most solutions utilized the following methods: the model predictive control method (MPC), the barrier Lyapunov functions (BLFs), and the nonlinear mapping functions (NMFs) [14, 15, 19, 25, 26, 28-31]. In [29], based on MPC and control allocation methods, a nonlinear control scheme was designed for a class of tilt-rotor vertical takeoff and landing aircraft. The proposed control method ensured the stability of the attitude error under symmetric attitude and velocity constraints. In [30], a dynamic model for a tilt-rotor UA was established and a trajectory-tracking control law using the MPC method was designed to ensure that the constrained states never violate the specified constraint range during flight. However, the MPC approach places significant demands on onboard computational resources especially when there are several constraint conditions [25]. To this end, some works have implemented the BLFs to tackle the issue of state constraints for aircraft [25, 31]. Nevertheless, the BLF method introduces considerable additional complexity in control law design [32]. In contrast, NMFs map constrained states onto the real number set, thereby transforming the state constraint problem into ensuring the boundedness of the transformed signals. Since the NMF method can significantly simplify the control law design process while ensuring that constraints are not violated, numerous control algorithms based on this method have been proposed. Studies such as [14, 15, 19, 26, 28] proposed control methods for hypersonic vehicles, quadrotors, spacecraft, and FW UA swarms with state constraints based on the NMF approach. However, the NMFs presented in [14, 15, 19, 26, 28] can not be directly applied to the airspeed constraint problem, as it suffers from asymmetric magnitude restrictions. Besides, only part of the above works have achieved the finite-time (FINT) convergence, implying that the converge time is infinite [19, 28].

It is advantageous to deploy a FINT control algorithm for a dynamic system since it provides improved disturbance rejection capability and more precise steady-state performance [19, 28]. In the past few decades, researchers have put forward numerous FINT control approaches [17, 27, 31, 33]. FINT attitude control approaches for aircraft have been proposed in recent years; however, few attention has been paid to the attitude control problem for FW UA with angular velocity and AIS constraints taking effect simultaneously. Therefore, it is desirable to derive an advanced FINT attitude control method for FW UA under multiple constraints, which motivates the control algorithm presented in this paper.

This work studies the waypoint tracking problem for 6-DOF FW UA under the aforementioned constraints. The innovations and contributions are stated as follows.

- By applying the unit quaternion to describe the attitude of the 6-DOF FW UA, the problem of gimbal lock– unaddressed in [16, 18, 27]– is effectively avoided.
- The constraints imposed on the actuators and the angular velocity are explicitly considered and addressed through a developed smooth first-order AIS model affine in the model input and an NMF. This feature has not been addressed by most existing FW UA control methods [14, 16, 19, 20, 27, 31, 33, 34]. Besides, the AIS model can be deployed to other classes of dynamic systems that are subject to AIS.
- Different from the studies that focus on stabilizing attitude tracking errors in the body-fixed or wind coordinate systems [16, 18, 27, 35], this work proposes an attitude control approach for the ballistic coordinate system of the FW UA via a novel defined attitude error, which means the direction of motion in the inertia frame can be regulated. Then, the waypoint tracking mission for the underactuated UA subject to multiple constraints, external disturbances, and unknown composite wind can be accomplished.

The remainder of this article are organized as follows. Section 2 provides needed preliminaries, brief description of the dynamics of the aircraft, and problem statement. Section 3 describes the FINT attitude control design for the UA and stability analysis. Simulation results are put forward in Section 4, followed by conclusions in Section 5.

2. PRELIMINARIES

2.1. Notations

Throughout this article, the following notations will be used. F^n, F^b, F^B, and F^w respectively represent

the inertial frame, the body-fixed frame, the ballistic frame, and the wind frame of a 6-DOF FW UA. The induced norm of a matrix or the Euclidean norm of a vector is denoted by $\|\cdot\|$. Given $\varpi \in \mathbb{R}^3$, $\mathcal{G}(\varpi)$ represents the cross-product operator. $\odot$ denotes the quaternion multiplication. For $\varpi \in \mathbb{R}^n$ and a positive number β, denote $\varpi^\beta = col(\varpi_1^\beta, \cdots, \varpi_n^\beta)$, where $col(\varpi_1, \cdots, \varpi_n) = [\varpi_1, \cdots, \varpi_n]^T$. Let $sig^\alpha(\varpi) = col(sig^\alpha(\varpi_1), \ldots, sig^\alpha(\varpi_n))$, where $sig^\alpha(x) = |x|^\alpha sign(x)$ for $\alpha \in (0,1)$, and $sign(\cdot)$ denotes the signum function with $sign(0) = 0$. I_n refers to the $n \times n$ identity matrix. $\mathbb{R}^+$ represents the set of positive real numbers. $\lambda_{max}(\cdot)$ refers to the maximum eigenvalue and $\lambda_{min}(\cdot)$ denotes the minimum eigenvalue of a matrix, respectively.

2.2. Necessary Lemmas

Consider the following system:

$$\dot{x} = f(x,t), \quad f(0,t) = 0, \quad x(0) = x_0, \quad x \in U \subset \mathbb{R}^n, \tag{1}$$

where the nonlinear function $f: U \times \mathbb{R}^+ \to \mathbb{R}^n$ is continuous in an open neighborhood U of the origin $x = 0$.

Definition 1 [36] If there exists an open neighborhood of the origin $U_0 \subset U$ and a function $\mathcal{T}(x_0): U_0 \setminus \{0\} \to (0, \infty)$ such that, for all $x_0 \in U_0$, the solution $s(t, x_0) \in U_0 \setminus \{0\}$ exists for $t \in [0, \mathcal{T}(x_0))$ and satisfies

$$\lim_{t \to \mathcal{T}(x_0)} s(t, x_0) = 0,$$

then $\mathcal{T}(x_0)$ is called the settling time, and the zero solution of system (1) is said to be locally FINT convergent. If the zero solution of system (1) is FINT convergent, the set of all x_0 such that $s(t, x_0) \to 0$ is called the domain of attraction of the solution. Furthermore, if $U = U_0 = \mathbb{R}^n$, then the zero solution of the system is globally FINT stable.

Lemma 1 [35, 37] Consider a Lyapunov function $V(x,t)$ defined on $U_1 \times \mathbb{R}^+$, where $U_1 \subseteq U \subset \mathbb{R}^n$ is a neighborhood of the origin, and suppose that

$$\dot{V}(x,t) \le -lV^a(x,t) - kV(x,t), \quad \forall x \in U_1 \setminus \{0\}, \tag{2}$$

where $l, k > 0$ and $0 < a < 1$. Then, the origin of system (1) is locally FINT stable. For $x(t_0) \in U_1$, the settling time satisfies

$$\mathcal{T}(x_0) \le \frac{1}{k(1-a)} \ln\left(\frac{kV^{1-a}(x_0) + l}{l} \right).$$

Lemma 2 [38] For $\alpha_i \in \mathbb{R}\ (i = 1, 2, \ldots, m)$ and $0 < \gamma < 1$, the following inequality holds:

$$\left(\sum_{i=1}^{m} |\alpha_i| \right)^\gamma \le \sum_{i=1}^{m} |\alpha_i|^\gamma .$$

Lemma 3 [27] For $\gamma \in (0,1)$ and any $\varpi \in \mathbb{R}$, define the function $sigM(\varpi, \gamma)$ as

$$sigM(\varpi,\gamma) = \begin{cases} sig^\gamma(\varpi) + sign(\varpi)\left(k + (\gamma - 1)\delta^\gamma\right), & |\varpi| > \delta, \\ \gamma \delta^{\gamma - 1} \varpi + k \sin\left(\frac{\pi}{2} \frac{\varpi}{\delta} \right), & |\varpi| \le \delta, \end{cases}$$

where $sig^\gamma(\varpi) = |\varpi|^\gamma sign(\varpi)$ and the parameters $\delta > 0$ and $k > 0$ satisfy $k > (1 - \gamma)\delta^\gamma$. Then, the following inequality holds:

$$\varpi\left(sig^\gamma(\varpi) - sigM(\varpi,\gamma) \right) < \delta^{\gamma+1}. \tag{3}$$

For the vector $\varpi = col(\varpi_1, \varpi_2, \ldots, \varpi_n) \in \mathbb{R}^n$, define

$$sigM(\varpi,\gamma) = col(sigM(\varpi_1,\gamma), \ldots, sigM(\varpi_n,\gamma)),$$

and

$$sig^\gamma(\varpi) = col(sig^\gamma(\varpi_1), sig^\gamma(\varpi_2), \ldots, sig^\gamma(\varpi_n)).$$

Lemma 4 [39] The following inequality holds for any $\iota > 0$ and for any $\Phi \in R$

$$0 \le |\Phi| - \Phi \tanh\left(\frac{k_s \Phi}{\iota} \right) \le \iota,$$

where k_s is a constant that satisfies $k_s = e^{-(k_s + 1)}$, i.e., $k_s = 0.2785$.

Remark 1 for any $\Phi = col(\Phi_1, \ldots, \Phi_n) \in \mathbb{R}^n$, by using Lemma 4, the following inequality holds:

$$\left| \|\Phi\| - \Phi \tanh\left(\frac{n k_s \Phi}{\iota} \right) \right| \le \sum_{i=1}^{n} \left(|\Phi_i| - \Phi_i \tanh\left(\frac{n k_s \Phi_i}{\iota} \right) \right) \le \iota \tag{4}$$

Lemma 5 [40] For any real variables z, α and $\mu > 0$, $\upsilon > 0$, and $\varepsilon > 0$, the following inequality holds:

$$|z|^\mu |\alpha|^\upsilon \le \frac{\mu}{\mu + \upsilon} \varepsilon |z|^{\mu + \upsilon} + \frac{\upsilon}{\mu + \upsilon} \varepsilon^{-\frac{\mu}{\upsilon}} |\alpha|^{\mu + \upsilon}.$$

2.3. Dynamics of the 6-DOF FW UA

Before presenting the dynamics of the FW UA under consideration, several necessary assumptions are made to simplify the analysis of the flight process.

Assumption 1 The motion of the aircraft is assumed to satisfy the following conditions:

1. The aircraft mass is considered constant;
2. The FW UA is considered as a rigid body, and elastic motions of its structure caused by external forces during flight are neglected;
3. The UA operates within a certain altitude range, such that variations in gravitational acceleration are neglected.

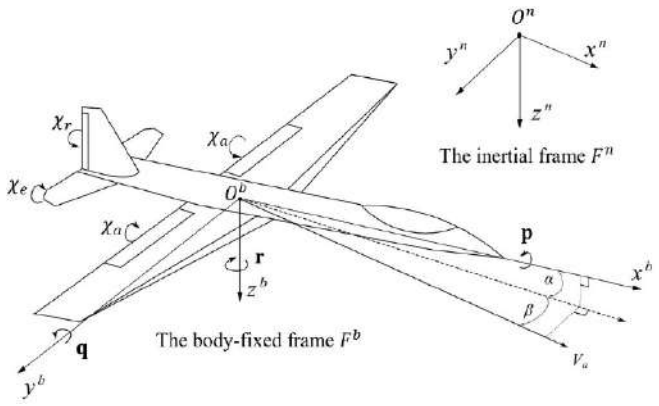

Figure 1: Coordinate systems of the FW UA.

The dynamics of the considered 6-DOF FW UA can be described by [7, 41]

$$\dot{p}^n = \mathbf{R}_b^n \nu^b$$

$$\dot{\nu}_r^b = \frac{1}{m}\mathbf{f}_{Th}^b + \frac{1}{m}\mathbf{R}_w^b \mathbf{f}_a^w + \mathbf{R}_n^b \mathbf{f}_g^n - \mathcal{S}(\omega_{nb}^b)\nu_r^b + d_v$$

$$\dot{q}_{nb} = \frac{1}{2} q_{nb} \odot col(0, \omega_{nb}^b)$$

$$\mathbf{J}\dot{\omega}_{nb}^b = -\mathcal{S}(\omega_{nb}^b)\mathbf{J}\omega_{nb}^b + \mathbf{f}(\alpha,\beta) - \mathcal{D}\omega_{nb}^b + \mathcal{B}\chi_\tau + d_\omega \qquad (5)$$

where p^n is the position vector of the FW UA, $\nu^b = \mathbf{R}_b^n \nu_r^b + \nu_{wind}^n$ is the ground velocity vector of the center of mass, $\nu_r^b = col(u,v,w)$ represents the airspeed of the body frame relative the wind vector ν_{wind}^n, m is the mass, $\mathbf{f}_{Th}^b = col(\chi_T, 0, 0)$ is the thrust vector with χ_T being the thrust, and $\mathbf{f}_g^n = col(0,0,g)$ is the gravity vector where g is the gravitational acceleration. For the rotational subsystem, q_{nb} is the unit quaternion which is utilized to parameterize the orientation of the FW UA, $\omega_{nb}^b = col(\mathbf{p},\mathbf{q},\mathbf{r})$ denotes the angular velocity of F^b relative to F^n referenced in F^b, $\mathbf{J}$ is the moment of inertia, $\chi_\tau = col(\chi_a, \chi_e, \chi_r) \in \mathbb{R}^3$ denotes the deflection of control surfaces, and d_v and d_ω respectively denote the bounded unknown external disturbances applied to the position and attitude subsystem. The matrix $\mathbf{R}_n^b$ denotes the rotation matrix formed as

$$\mathbf{R}_b^n = \mathbf{I}_3 + 2q_{nb0}\overline{q}_{nb}^\times + 2\overline{q}_{nb}^\times \overline{q}_{nb}^\times$$

The rotation matrix from body to wind is defined as

$$\mathbf{R}_b^w = \begin{bmatrix} c\alpha c\beta & s\beta & s\alpha c\beta \\ -c\alpha s\beta & c\beta & -s\alpha s\beta \\ -s\alpha & 0 & c\alpha \end{bmatrix}$$

where $c(\cdot)$ and $s(\cdot)$ denote $\cos(\cdot)$ and $\sin(\cdot)$, respectively, and the attack angle α and sideslip angle β are respectively defined by $\alpha = \arctan(\frac{w}{u})$ and $\beta = \arcsin(\frac{v}{V_a})$, where V_a is the airspeed defined as $V_a = \left\| \nu_r^b \right\|$. The aerodynamic forces and moments are defined as

$$\mathbf{f}_a^w = \frac{1}{2}\rho S_w V_a^2 \begin{bmatrix} -C_D \\ C_{Y_\beta}\beta \\ -C_L \end{bmatrix}$$

$$C_D = C_{D_0} + C_{D_{\tau e}}\chi_e + C_{D_{\tau r}}\chi_r + \frac{C_L - C_{L_{min}}}{\pi e AR}$$

$$C_Y = C_{Y_\beta}\beta + C_{Y_{\tau r}}\chi_r + \frac{b}{2V_a}(C_{Y_p}\mathbf{p} + C_{Y_r}\mathbf{r})$$

$$C_L = C_{L_0} + C_{L_\alpha}\alpha + C_{L_{\tau e}}\chi_e + \frac{\overline{c}}{2V_a}(C_{L_q}\mathbf{q} + C_{L_{\dot{\alpha}}}\dot{\alpha})$$

$$\mathbf{f}(\alpha,\beta) = \frac{1}{2}\rho S_w V_a^2 \begin{bmatrix} b(C_{l_\beta}\beta) \\ \overline{c}(C_{m_0} + C_{m_\alpha}\alpha) \\ b(C_{n_\beta}\beta) \end{bmatrix}$$

The matrices $\mathcal{D}$ and $\mathcal{B}$ are respectively defined by

$$\mathfrak{D} = -QS_w \begin{bmatrix} \frac{b^2}{2V_a}C_{l_p} & 0 & \frac{b^2}{2V_a}C_{l_r} \\ 0 & \frac{\overline{c}^2}{2V_a}C_{m_q} & 0 \\ \frac{b^2}{2V_a}C_{n_r} & 0 & \frac{b^2}{2V_a}C_{n_r} \end{bmatrix}$$

$$\mathfrak{B} = \begin{bmatrix} QS_w bC_{l\tau a} & 0 & QS_w bC_{l\tau r} \\ 0 & QS_w \overline{c}C_{m\tau e} & 0 \\ QS_w bC_{n\tau a} & 0 & QS_w bC_{n_{\tau r}} \end{bmatrix}$$

where $Q = \frac{1}{2}\rho V_a^2$ and the details of $C_{\Delta\Delta}$ are shown in Section 4.

By differentiating the airspeed V_a along time, one deduces the translational subsystem as

$$\dot{V}_a = \frac{\boldsymbol{\nu}_r^{bT}}{V_a}\left(\frac{1}{m}\mathbf{f}_{T_h}^b + \frac{1}{m}\mathbf{R}_w^b\mathbf{f}_a^w + \mathbf{R}_n^b\mathbf{f}_g^n\right) + d_V \tag{6}$$

where $d_V = \frac{\nu_r^{bT}}{V_a}d_v \in \mathbb{R}$ is the bounded unknown disturbance applied to the translational subsystem.

Assumption 2 The disturbances d_v and d_ω, together with their first derivatives, are unknown but bounded.

Assumption 3 Due to the constraints on UA velocities and control inputs, it is assumed that there exist known constants $\mathbf{p}_M > 0$, $\mathbf{p}_m > 0$, $\mathbf{q}_M > 0$, $\mathbf{q}_m > 0$, $\mathbf{r}_M > 0$, $\mathbf{r}_m > 0$, $\chi_{jM} > 0$, and χ_{jm} (with $\chi_{jm} = 0.05\chi_{jM} > 0$ when $j = T$ and $\chi_{jm} < 0$ when $j = a,e,r$), such that $-\mathbf{p}_m < \mathbf{p} < \mathbf{p}_M$, $-\mathbf{q}_m < \mathbf{q} < \mathbf{q}_M$, $-\mathbf{r}_m < \mathbf{r} < \mathbf{r}_M$, and $\chi_{jm} < \chi_j < \chi_{jM}$ for $j \in \{T,a,e,r\}$. For the attitude or airspeed commands, there exists a control input sequence that satisfies the AIS constraints, such that under this control law, the FW UA states can track the given commands.

Remark 2 Assumption 1, which has been shown to be sufficiently accurate for describing aircraft motion, is widely employed in FW UA attitude control approaches [27, 42]. During flight, disturbances affect the UA's performance persistently. Since excessive disturbances may cause loss of control, it is reasonable to assume that disturbances are bounded, as stated in Assumption 2. Because AIS may prevent the tracking of arbitrary commands, Assumption 3 requires that the command be chosen such that a input exists to achieve tracking under AIS. Therefore, Assumption 3 is reasonable.

2.4. The Desired Attitude and Control Objective

The ground velocity $\dot{p}^n$, which is the actual flight direction in F^n, can be influenced by the attitude of the FW UA. A waypoint is often designated to the FW UA in most practical scenarios, such that the control system acquires the necessary information for the aircraft to execute attitude maneuvers and subsequently arrives at the specified waypoint and undertakes tasks. Represent the desired ballistic frame as F^d and denote the waypoint sequence as $p_d^n = [p_d^n(1),\ldots,p_d^n(i)] \in \mathbb{R}^{3\times i}$, where i denotes the number of waypoints. For the purpose of regulating the flight direction, the desired attitude for F^B parameterized by a unit quaternion, inspired by [7], is defined as $q_{nd} = col(\mathrm{q}_{nd}, \overline{q}_{nd})$ where $\mathrm{q}_{nd} = \cos(\frac{\rho}{2})$, $\overline{q}_{nd} = \mathrm{t}\sin(\frac{\rho}{2})$, $\rho = \arccos\left(\frac{\varepsilon_d \cdot \varepsilon_n}{\|\varepsilon_d\|\|\varepsilon_n\|}\right)$, $\mathrm{t} = \frac{\mathfrak{S}(\varepsilon_d)\varepsilon_n}{\|\mathfrak{S}(\varepsilon_d)\varepsilon_n\|}$, $\varepsilon_d = col(\|p_d^n(k) - p^n\|, 0, 0)$, and $\varepsilon_n = p_d^n(k) - p^n$ with $p_d^n(k)$ being the k th waypoint. It follows that the x-axis of F^d always coincides with the vector ε_n. Then, by using q_{nd}, the attitude tracking error can be defined by $q_e = q_{nd}^{-1} \odot q_{nB} = col(q_{e0}, \overline{q}_e)$, whose dynamic equations are given by

$$\dot{q}_e = \frac{1}{2}A(q_e)\omega_e(\omega_x), \dot{\omega}_x = \frac{\partial\omega_x}{\partial\omega_{nb}^b}\dot{\omega}_{nb}^b \tag{7}$$

where $A(q_e) = [-\overline{q}_e^T; q_{e0}\mathbf{I}_3 + \mathfrak{S}(\overline{q}_e)]$, $q_{nB} = q_{nb} \odot q_{bB} = col(q_{nB0}, \overline{q}_{nB})$, $q_{nB0} = \cos(\theta_{nB}/2)$, $\overline{q}_{nB} = t_{nB}\sin(\theta_{nB}/2)$, $\theta_{nB} = acos\left(\frac{\boldsymbol{\nu}^b \cdot col(1,0,0)}{\|\boldsymbol{\nu}^b \cdot col(1,0,0)\|}\right)$, $t_{nB} = \frac{\mathfrak{S}(\boldsymbol{\nu}^b)col(1,0,0)}{\|\mathfrak{S}(\boldsymbol{\nu}^b)col(1,0,0)\|}$, $\boldsymbol{\nu}^b = \mathbf{R}_n^b\dot{p}^n$, $\omega_e = \mathbf{R}_b^B\varphi_\omega(\omega_x, \omega_M, \omega_m) - \mathbf{R}_d^B\omega_{nd}^d + \omega_{bB}^B = \omega_x + f_q$ is a function of ω_x, $f_q = \mathbf{R}_b^B\varphi_\omega(\omega_x, \omega_M, \omega_m) - \mathbf{R}_d^B\omega_{nd}^d + \omega_{bB}^B - \omega_x$ is a nonlinear function that satisfies $\zeta_q \geq \|f_q\|_\infty$ with ζ_q being a positive constant, ω_{nd}^d represents the desired angular velocity expressed in the frame F^d, and ω_{bB}^B denotes the angular velocity of the ballistic frame F^B with respect to the body frame F^b, expressed in F^B.

Control Objective. The control objective is to achieve the waypoint tracking mission for the FW UA by aligning the ballistic frame F^B with the desired frame F^d via a FINT attitude control technique. Consequently, the UA can reach the designated waypoints under multiple constraints and thereby enabling the performing of various tasks such as target detection, object tracking, and aerial photography.

Remark 3 The attitude error defined in this study characterizes the difference between the desired frame F^d and the ballistic frame F^B. Distinct from conventional attitude error definitions based on the bodyâ€“desired frame difference (e.g., [16, 18, 27]), the stabilizing of the proposed attitude error $\overline{q}_e$ aligns the ground velocity with the active waypoint direction, resulting in a larger velocity component along the bodyâ€“target axis and thus enhancing both the speed and accuracy of waypoint tracking.

2.5. The First-Order AIS Model

A FW UA commonly suffers from the input nonlinearities including asymmetric/symmetric AIS. Control effectiveness can be fiercely decreased if the AIS constraint is not countered when designing a control algorithm. In this section, we address the issue of AIS applied to the inputs of both subsystems.

The first-order AIS model inspired by the works [34] is designed as

$$\dot{\chi} = \mathcal{G}\mathcal{U} - \gamma_u\left(\chi - \frac{\chi_m + \chi_M}{2}\right), \quad \chi_j(0) \in (\chi_{jm}, \chi_{jM})$$

where $\chi = col(\chi_T, \chi_\tau)$ is the output of the AIS model, $\mathcal{U} = col(u_\tau, u_\tau) = col(u_T, u_a, u_e, u_r) \in \mathbb{R}^4$ being the model input, $\chi_m = col(\chi_{Tm}, \chi_{am}, \chi_{em}, \chi_{rm})$, and $\chi_M = col(\chi_{TM}, \chi_{aM}, \chi_{eM}, \chi_{rM})$. The matrix $\mathcal{G}$ is defined as $\mathcal{G} = diag\{\mathcal{G}_T, \mathcal{G}_\tau^T\}$, where $\mathcal{G}_\tau = col(\mathcal{G}_a, \mathcal{G}_e, \mathcal{G}_r)$, and $\mathcal{G}_j$ ($j = T, a, e, r$) is given by $\mathcal{G}_j = -\frac{4}{(\chi_{jM} - \chi_{jm})^2}(\chi_j - \chi_{jm})(\chi_j - \chi_{jM})$. Clearly, if $\chi_j \in (\chi_{jm}, \chi_{jM})$, then $\mathcal{G}_j \in (0,1)$. The matrix γ_u is defined by $\gamma_u = diag\{\gamma_{uT}, \gamma_{ua}, \gamma_{ue}, \gamma_{ur}\} = diag\{\gamma_T, \gamma_\tau, \gamma_\tau, \gamma_\tau\}$ with γ_T and γ_τ both being sufficiently small constants.

Theorem 1 Consider the first-order AIS model (8). If the input u_j of model (8) remains bounded for $t > 0$, $\chi_j(0) \in (\chi_{jm}, \chi_{jM})$, then the model output χ_j can be restricted to satisfy the AIS constraint, i.e., $\chi_{jm} < \chi_j < \chi_{jM} (j = T, a, e, r)$.

Proof. See 6.

Remark 4 Unlike the input saturation model presented in [34], which captures only the symmetric saturation property of the actuation components, the proposed smooth AIS model characterizes both symmetric and asymmetric input saturation nonlinearities. This feature enables control design for various types of practical input-saturated systems even if they are exposed to AIS fault, thereby improving the applicability in engineering practice of the designed AIS model.

By implementing the designed AIS model (8), it can be guaranteed that the designed inputs for the FW UA follow the AIS constraints. Before proceeding with the control design, the problem of velocity constraints must first be addressed.

2.6. The Nonlinear Mapping Function and Constraint-Free System

Due to structural strength limitations of the airframe materials (e.g., wing bending-torsion deformation limits) and safety requirements of flight missions (e.g., aerial photography stability or payload protection), the body angular velocity of the UA must satisfy a certain limit. In this paper, it is assumed that the body angular velocity of the UA is subject to symmetric magnitude constraint. The angular velocity constraint is subsequently handled using an NMF formed as

$$\begin{aligned}\omega_{xj} &= \varphi_\omega^{-1}\left(\omega_{nb}^b(j), \omega_{jM}, \omega_{jm}\right) \\ &= \tfrac{1}{2}\ln\left(\frac{\omega_{jM}}{\omega_{jm}}\frac{\omega_{jM} + \omega_{jm}}{\omega_{jM} - \omega_{nb}^b(j)} - \frac{\omega_{jM}}{\omega_{jm}}\right),\end{aligned} \tag{8}$$

$$\begin{aligned}\omega_{nb}^b(j) &= \varphi_\omega\left(\omega_{xj}, \omega_{jM}, \omega_{jm}\right) \\ &= \frac{\omega_{jM}\omega_{jm}\left(e^{\omega_{xj}} - e^{-\omega_{xj}}\right)}{\omega_{jM}e^{-\omega_{xj}} + \omega_{jm}e^{\omega_{xj}}}, \quad j = 1,2,3,\end{aligned} \tag{9}$$

where $\omega_x = col(\omega_{x1}, \omega_{x2}, \omega_{x3}) \in \mathbb{R}^3$ is the unconstrained variable obtained after the nonlinear transformation of ω_{nb}^b, $\varphi_\omega(\cdot)$ denotes the transformation function, the vector ω_{nb}^b can be expressed as

$$\omega_{nb}^b = \varphi_\omega(\omega_x) = col\left(\varphi_\omega(\omega_{x1}), \varphi_\omega(\omega_{x2}), \varphi_\omega(\omega_{x3})\right),$$

and the lower and upper bounds of angular velocity are given by

$\omega_m = col(\omega_{1m}, \omega_{2m}, \omega_{3m}) = col(\mathbf{p}_m, \mathbf{q}_m, \mathbf{r}_m) \in \mathbb{R}^{3+}$,

$\omega_M = col(\omega_{1M}, \omega_{2M}, \omega_{3M}) = col(\mathbf{p}_M, \mathbf{q}_M, \mathbf{r}_M) \in \mathbb{R}^{3+}$,

with all elements being positive constants. Then, taking the time derivative of ω_x yields

$$\dot{\omega}_x = \frac{\partial \omega_x}{\partial \omega_{nb}^b} \dot{\omega}_{nb}^b$$

$$= \frac{\partial \omega_x}{\partial \omega_{nb}^b} (-\mathbf{J}^{-1} \mathfrak{S}(\omega_{nb}^b) \mathbf{J} \omega_{nb}^b + \mathbf{J}^{-1} \mathbf{f}(\alpha, \beta)$$

$$-\mathbf{J}^{-1} \mathfrak{D} \omega_{nb}^b + \mathbf{J}^{-1} \mathfrak{B} \chi_\tau + \mathbf{J}^{-1} d_\omega) \tag{10}$$

$$\frac{\partial \omega_x}{\partial \omega_{nb}^b} = diag\{\frac{\partial \omega_{x1}}{\partial \mathbf{p}}, \frac{\partial \omega_{x2}}{\partial \mathbf{q}}, \frac{\partial \omega_{x3}}{\partial \mathbf{r}}\} \tag{11}$$

$$\frac{\partial \omega_{xj}}{\partial \omega_{nb}^b(j)} = \frac{1}{2} \frac{\omega_{jM} + \omega_{jm}}{(\omega_{jm} + \omega_{nb}^b(j))(\omega_{jM} - \omega_{nb}^b(j))} > 0 \tag{12}$$

It can be observed that as long as the transformed angular velocities ω_{x1}, ω_{x2}, and ω_{x3} remain bounded, the terms $\frac{\partial \omega_{x1}}{\partial \mathbf{p}}$, $\frac{\partial \omega_{x2}}{\partial \mathbf{q}}$, and $\frac{\partial \omega_{x3}}{\partial \mathbf{r}}$ are all strictly positive and its intuitive that ω_{nb}^b does not violate the constraint conditions.

Remark 5 By applying the proposed AIS model (8) and the NMF (9) to the FW UA system given by (5), one deduces

$$\dot{p}^n = \mathbf{R}_b^n v^b$$

$$\dot{V}_a = \frac{\nu_r^{bT}}{V_a} (\frac{\chi_T}{m} + \frac{1}{m} \mathbf{R}_w^b \mathbf{f}_a^w + \mathbf{R}_n^b \mathbf{f}_g^n) + d_V$$

$$\dot{\chi}_T = \mathfrak{G}_T u_T - \gamma_T \left(\chi_T - \frac{\chi_{TM} + \chi_{Tm}}{2} \right)$$

$$\dot{q}_{nb} = \frac{1}{2} q_{nb} \odot col(0, \varphi_\omega(\omega_x, \omega_M, \omega_m))$$

$$\dot{\omega}_x = \frac{\partial \omega_x}{\partial \omega_{nb}^b} (-\mathbf{J}^{-1} \mathfrak{S}(\omega_{nb}^b) \mathbf{J} \omega_{nb}^b + \mathbf{J}^{-1} \mathbf{f}(\alpha, \beta)$$

$$-\mathbf{J}^{-1} \mathfrak{D} \omega_{nb}^b + \mathbf{J}^{-1} \mathfrak{G} \chi_\tau + \mathbf{J}^{-1} d_\omega)$$

$$\dot{\chi}_\tau = \mathfrak{G}_\tau u_\tau - \gamma_\tau \left(\chi_\tau - \frac{\chi_{\tau M} + \chi_{\tau m}}{2} \right) \tag{13}$$

By designing a FINT attitude control law for the unconstrained system (13), the desired attitude of the FW UA can be realized in a finite time with the considered mixed-constraints being agreed.

3. MAIN RESULTS

In this section, on the basis of the referenced airspeed and attitude command q_{nd}, the FINT airspeed and attitude control algorithm for the FW UA under multiple constraints is derived by virtue of the designed AIS model, an introduced FINT disturbance observer, the backstepping technique, and the FINT control method.

3.1. The FINT Airspeed Control Law

The airspeed needs to track the prescribed command $V_d \in (V_m, V_M)$ during flight and hence avoids introducing additional control requirements for stabilizing attitude error. To this effect, a control law for the translational subsystem is designed in the sequel.

Step 1: Design of a virtual controller for χ_T.

Define the airspeed tracking error $e_V = V_a - V_d$ and $e_T = \chi_T - \chi_{Td}$, where χ_{Td} is the virtual controller for χ_T. The dynamic equation for e_V is given by

$$\dot{e}_V = \frac{u}{m V_a} \chi_T + \frac{\nu_r^{bT}}{V_a} (\frac{1}{m} \mathbf{R}_w^b \mathbf{f}_a^w + \mathbf{R}_n^b \mathbf{f}_g^n) + f_V \tag{14}$$

where $f_V = d_V - \dot{V}_d$ is the lumped nonlinear uncertainty that satisfies $\sup_{t>0}\{f_V\} \le \xi_V$, with ξ_V being a positive constant.

Consider the Lyapunov candidate $\mathbf{W}_V = \frac{1}{2} e_V^2 + \frac{1}{2} \lambda_{V1} \tilde{\xi}_V^{\,2}$, where $\lambda_{V1} > 0$ and $\tilde{\xi}_V = \hat{\xi}_V - \xi_V$ with $\hat{\xi}_V$ being the estimate of ξ_V. Taking the time derivative of $\mathbf{W}_V$ yields

$$\dot{\mathbf{W}}_V = e_V (\frac{u}{m V_a} \chi_T + \frac{\nu_r^{bT}}{V_a} (\frac{1}{m} \mathbf{R}_w^b \mathbf{f}_a^w + \mathbf{R}_n^b \mathbf{f}_g^n) + f_V) + \lambda_{V1} \tilde{\xi} \dot{\tilde{\xi}} \tag{15}$$

The virtual controller χ_{Td} can now be designed as

$$\chi_{Td} = \frac{m V_a}{u} (-\frac{\nu_r^{bT}}{V_a} \left(\frac{1}{m} \mathbf{R}_w^b \mathbf{f}_a^w + \mathbf{R}_n^b \mathbf{f}_g^n \right)$$

$$-\left(k_V e_V + k_V sigM(e_V, \Gamma_0) + \psi_V \right)) \tag{16}$$

$$\psi_V = \hat{\xi}_V \tanh\left(\frac{k_s e_V \hat{\xi}_V}{\iota} \right) \tag{17}$$

$$\dot{\hat{\xi}}_V = \frac{1}{\lambda_{V1}} | e_V | - \frac{\lambda_{V2}}{\lambda_{V1}} \hat{\xi}_V \tag{18}$$

where ψ_V is a robust term, $\iota > 0$ is a small constant, $\dot{\hat{\xi}}_V$ is the adaptive law, $\Gamma_0 \in (0,1)$, $k_V > 0$, and $\lambda_{V2} > 0$ is positive constant to be chosen.

Considering Lemma 3, Lemma 4, Lemma 5, and the inequality

$$-\lambda_{V2}\hat{\xi}_V\tilde{\xi}_V = -\lambda_{V2}\tilde{\xi}_V\left(\tilde{\xi}_V + \xi_V\right)$$

$$\leq -\frac{\lambda_{V2}}{2}\tilde{\xi}_V{}^2 + \frac{\lambda_{V2}}{2}\xi_V^2$$

$$\leq -\lambda_{V2}\left(\frac{1}{2k}\tilde{\xi}_V{}^2 + \frac{1}{2-2k}\tilde{\xi}_V{}^2 + \frac{1}{2k}(1-l)l^{\frac{l}{1-l}} - \frac{1}{2k}(1-l)l^{\frac{l}{1-l}}\right)$$

$$+\frac{\lambda_{V2}}{2}\xi_V^2$$

$$\leq \frac{\lambda_{V2}}{2}\xi_V^2 + \frac{1}{2k}\lambda_{V2}(1-l)l^{\frac{l}{1-l}} - \frac{1}{2k}\frac{\lambda_{V2}}{2^{l-1}}\frac{1}{2}\tilde{\xi}_V{}^{2l} - \frac{\lambda_{V2}}{2-2k}\tilde{\xi}_V^2 \tag{19}$$

with $k, l = \frac{1+\Gamma_0}{2} \in (0,1)$ representing some positive constant, substitution of (16) into (15) yields

$$\dot{\mathbf{W}}_V = \frac{u}{mV_a}e_V e_T + e_V\left(\frac{u}{mV_a}\chi_{Td} + \frac{\boldsymbol{\nu}_r^{bT}}{V_a}\left(\frac{1}{m}\mathbf{R}_w^b\mathbf{f}_a^w + \mathbf{R}_n^b\mathbf{f}_a^n\right) + f_V\right) + \lambda_{V1}\tilde{\xi}\dot{\hat{\xi}}$$

$$\leq \frac{u}{mV_a}e_V e_T - k_V e_V^2 - k_V e_V\, sigM(e_V, \Gamma_0) - e_V\hat{\xi}_V \tanh\left(\frac{k_s e_V \hat{\xi}_V}{\iota}\right)$$

$$+\hat{\xi}_V | e_V | - \lambda_{V2}\hat{\xi}_V^2 + \lambda_{V2}\hat{\xi}_V\xi_V$$

$$\leq \frac{u}{mV_a}e_V e_T - k_V e_V^2 - k_V e_V\, sig^{\Gamma_0}(e_V) + k_V\delta^{1+\Gamma_0} + \iota + \lambda_{V2}\xi_V^2$$

$$+\frac{\lambda_{V2}}{2k}(1-l)l^{\frac{l}{1-l}} - \frac{1}{2k}\frac{\lambda_{V2}}{2^{l-1}}\frac{1}{2}\tilde{\xi}_V{}^{2l}$$

$$\leq \frac{u}{mV_a}e_V e_T - k_V e_V^2 - k_V e_V\, sig^{\Gamma_0}(e_V) - \frac{2\lambda_{V2}}{(2-2k)\lambda_{V1}}\frac{1}{2}\lambda_{V1}\tilde{\xi}_V^2$$

$$-\frac{\lambda_{V2}}{2k\lambda_{V1}^l}\left(\frac{1}{2}\lambda_{V1}\tilde{\xi}_V^2\right)^l + \Delta_V$$

$$\leq \frac{u}{mV_a}e_V e_T - c_{V1}\mathbf{W}_V - c_{V2}\mathbf{W}_V^{\frac{1+\Gamma_0}{2}} + \Delta_V \tag{20}$$

where $c_{V1} = \min\left\{k_V, \frac{2\lambda_{V2}}{(2-2k)\lambda_{V1}}\right\}$, $c_{V2} = \min\left\{k_V, \frac{\lambda_{V2}}{2k\lambda_{V1}^l}\right\}$, $\Delta_V = \iota + \lambda_{V2}\xi_V^2 + \frac{\lambda_{V2}}{2k}(1-l)l^{\frac{l}{1-l}} + k_V\delta^{1+\Gamma_0}$ and the coupled term $\frac{u}{mV_a}e_V e_T$ will be addressed in the next step.

Step 2: Design of the control law for u_T.

Consider the Lyapunov function $\mathbf{W}_T = \frac{1}{2}e_T^2$. Taking the time derivative of $\mathbf{W}_T$ yields

$$\dot{\mathbf{W}}_T = e_T\left(\dot{\chi}_T - \dot{\chi}_{Td}\right)$$

$$= e_T(\mathfrak{G}_T u_T - \gamma_T\left(\chi_T - \frac{\chi_{Tm} + \chi_{TM}}{2}\right) - \dot{\chi}_{Td})$$

$$\leq e_T(u_T - u_T + \mathfrak{G}_T u_T - \gamma_T\left(\chi_T - \frac{\chi_{Tm} + \chi_{TM}}{2}\right) - \dot{\chi}_{Td})$$

$$\leq e_T\left(u_T - \gamma_T\left(\chi_T - \frac{\chi_{Tm} + \chi_{TM}}{2}\right) + f_T\right) \tag{21}$$

where $f_T = -u_T + \mathfrak{G}_T - \dot{\chi}_{Td}$ is the lumped uncertainty. To compensate the uncertain term f_T, a FINT observer is introduced as [34]

$$\begin{cases} \dot{\hat{e}}_T = \hat{f}_T + u_T - \gamma_T\left(\chi_T - \frac{\chi_{Tm} + \chi_{TM}}{2}\right) - \gamma_0\gamma_1\, sig^{\Gamma_1}(\tilde{e}_T) \\ \dot{\hat{f}}_T = -\gamma_0^2\gamma_2\, sig^{\Gamma_2}(\tilde{e}_T) \end{cases} \tag{22}$$

where $\hat{e}_T$ is the estimate of e_T with the estimate error being defined by $\tilde{e}_T = \hat{e}_T - e_T$ and $\hat{f}_T$ is the estimate of f_T with the estimate error being $\tilde{f}_T = \hat{f}_T - f_T$.

Lemma 6 [34] Consider the FINT disturbance observer of the form given in (22). For any positive constant f_{TM}, if the inequality $\left|\left|\dot{f}_T\right|\right| \leq f_{TM}$ holds, then there exists a sufficiently large observer parameter γ_0 such that the estimation error vector $E_{OT} = col(\tilde{e}_T, \tilde{f}_T)$ can converge to a sufficiently small set $\left|\left|E_{OT}\right|\right| \leq \Delta_{OT}$ within finite time, where Δ_{OT} is a small constant.

Remark 6 It is noticeable that extended state observer (ESO) and high-gain observer techniques can both achieve convergence of estimate errors. However, high-gain observer often introduces a trade-off between estimation performance and chattering due to its high-

gain property. In contrast, the ESO avoids the chattering problem, while the FINT convergence can not be ensured without additional design and analysis efforts, which increases the overall system complexity. Hence, the disturbance observer proposed in [34] is employed in our work to compensate for the lumped uncertainties such that the FINT convergence of the closed-loop system is ensured without excessive chattering.

Design the actual input for the AIS model u_T as

$$u_T = \gamma_T\left(\chi_T - \frac{\chi_{Tm}+\chi_{TM}}{2}\right) - \hat{f}_T - k_T(e_T + sig^{\Gamma_0}(e_T)) - \frac{u}{mV_a}e_V \quad (23)$$

where $k_T > 0$ is a constant. Substituting (23) into (21), one obtains

$$\dot{\mathbf{W}}_T \le e_T\tilde{f}_T - k_T e_T^2 - k_T e_T\, sig^{\Gamma_0}(e_T) - \frac{u}{V_a m}e_V e_T$$

$$\le \frac{1}{2}k_T e_T^2 + \frac{1}{2k_T}\tilde{f}_T^2 - k_T e_T^2 - \frac{u}{V_a m}e_V e_T - k_T \mathbf{W}_T^{\frac{1+\Gamma_0}{2}}$$

$$\le -\frac{u}{V_a m}e_V e_T - k_T\mathbf{W}_T - k_T\mathbf{W}_T^{\frac{1+\Gamma_0}{2}} + \Delta_T \quad (24)$$

where Young's inequality is utilized and Δ_T is a positive bounded constant satisfies $\Delta_T = \sup_{t>0}\{\frac{1}{2k_T}\tilde{f}_T^2\}$.

Lemma 7 Consider the translational subsystem defined by (6) and the AIS model (8). Suppose that Assumptions 1-3 hold. Let the control law be (23), where the virtual controller χ_{Td} is defined as (16), the FINT disturbance observer is given by (22). Provided that $\mathbf{W}_V(0)$ and $\mathbf{W}_T(0)$ are bounded. The designed control law can guarantee that the tracking error $E_T = col(e_V, e_T)$ can converge to a sufficiently small region near zero within a finite time interval with the AIS constraint being followed.

Proof. Consider the Lyapunov function $\mathbf{W}_p = \mathbf{W}_V + \mathbf{W}_T$, with $\mathbf{W}_p(0)$ being bounded. Taking the time derivative of $\mathbf{W}_p$ along (20) and (24) yields

$$\dot{\mathbf{W}}_p \le \frac{u}{mV_a}e_V e_T - k_V\mathbf{W}_V - k_V\mathbf{W}_V^{\frac{1+\Gamma_0}{2}} + \Delta_V$$

$$-\frac{u}{V_a m}e_V e_T - k_T\mathbf{W}_T + k_T\mathbf{W}_T^{\frac{1+\Gamma_0}{2}} + \Delta_T$$

$$\le -k_V\mathbf{W}_V - k_V\mathbf{W}_V^{\frac{1+\Gamma_0}{2}} + \Delta_V - k_T\mathbf{W}_T - k_T\mathbf{W}_T^{\frac{1+\Gamma_0}{2}} + \Delta_T$$

$$\le -K_V\mathbf{W}_p - K_V\mathbf{W}_p^{\frac{1+\Gamma_0}{2}} + \Delta_p \quad (25)$$

where $K_V = \min\{k_V, k_T\}$ and $\Delta_p = \Delta_V + \Delta_T$. Hence, E_T can converge to the region $\|E_T\| \le \Delta_{ET}$ within a finite time, where $\Delta_{ET} = \max\left\{\sqrt{\frac{\Delta_p}{K_V}}, \left(\frac{\Delta_p}{K_V}\right)^{\frac{1}{1+\Gamma_0}}\right\}$. With $\mathbf{W}_V(0)$ and $\mathbf{W}_T(0)$ both being bounded and $\dot{\mathbf{W}}_p < 0$ for $\|E_T\| > \Delta_{ET}$, it can be guaranteed that all the transformed signals are bounded for $t > 0$. This completes the proof.

Once airspeed tracking is achieved, it is more critical to stabilize the attitude errors, thereby enabling the UA to accomplish its assigned tasks more effectively.

3.2. The FINT Attitude Control Law

One of the most crucial procedures for achieving the control objective is the design of an attitude control algorithm capable of effectively stabilising attitude error q_e defined in (7). Hence, the FINT attitude control law is derived by using the backstepping technique in the sequel.

Step 1: Design of a virtual controller for ω_x.

Define the tracking error $\Omega_e = \omega_x - \omega_{xc}$, where ω_{xc} is the virtual controller for ω_x. Consider the Lyapunov candidate $\mathbf{W}_q = 2(1-q_{e0}) + \frac{1}{2}\lambda_{q1}\tilde{\xi}_q^2$, where $\lambda_{q1} > 0$ and $\tilde{\xi}_q = \hat{\xi}_q - \xi_q$ with $\hat{\xi}_q$ being the estimate of ξ_q. Taking the time derivative of $\mathbf{W}_q$ yields

$$\dot{\mathbf{W}}_q = \bar{q}_e^T\omega_e$$

$$= \bar{q}_e^T(\omega_x - \omega_x - \omega_{xc} + \omega_{xc} + \omega_e)$$

$$= \bar{q}_e^T(\Omega_e + \omega_{xc} + f_q) \quad (26)$$

The virtual controller ω_{xc} can now be designed as

$$\omega_{xc} = -\psi_q - k_q\left(\bar{q}_e + sigM(\bar{q}_e, \Gamma_0)\right) \quad (27)$$

$$\psi_q = \hat{\xi}_q \tanh\left(\frac{3k_s\hat{\xi}_q\bar{q}_e}{\iota}\right) \quad (28)$$

$$\dot{\hat{\xi}}_q = \frac{1}{\lambda_{q1}}\left\|\overline{q}_e\right\| - \frac{\lambda_{q2}}{\lambda_{q1}}\hat{\xi}_q \tag{29}$$

where ψ_q is a robust term, $\iota > 0$ is a small constant, $\dot{\hat{\xi}}_q$ is the adaptive law, $\Gamma_0 \in (0,1)$, $k_q > 0$, and $\lambda_{q2} > 0$ is positive constant to be chosen.

Considering Lemma 3, Lemma 4, Lemma 5, and the inequality

$$-\lambda_{q2}\hat{\xi}_q\tilde{\xi}_q = -\lambda_{q2}\tilde{\xi}_q\left(\tilde{\xi}_q + \zeta_q\right)$$

$$\le -\frac{\lambda_{q2}}{2}\tilde{\xi}_q^{\,2} + \frac{\lambda_{q2}}{2}\zeta_q^2$$

$$\le -\lambda_{q2}\left(\frac{1}{2k}\tilde{\xi}_q^{\,2} + \frac{1}{2-2k}\tilde{\xi}_q^{\,2} + \frac{1}{2k}(1-l)l^{\frac{l}{1-l}} - \frac{1}{2k}(1-l)l^{\frac{l}{1-l}}\right)$$

$$+\frac{\lambda_{q2}}{2}\zeta_q^2$$

$$\le \frac{\lambda_{q2}}{2}\zeta_q^2 + \frac{1}{2k}\lambda_{q2}(1-l)l^{\frac{l}{1-l}} - \frac{1}{2k}\frac{\lambda_{q2}}{2^{l-1}}\frac{1}{2}\tilde{\xi}_q^{\,2l} - \frac{\lambda_{q2}}{2k-2}\tilde{\xi}_q^2 \tag{30}$$

with $k,l = \frac{1+\Gamma_0}{2} \in (0,1)$ representing some positive constant, substitution of (16) into (15) yields

$$\dot{\mathbf{W}}_q = \overline{q}_e^T\Omega_e - k_q\overline{q}_e^T\overline{q}_e - k_q\overline{q}_e^T sigM(\overline{q}_e,\Gamma_0) + \overline{q}_e^T f_q - \overline{q}_e^T\psi_q + \lambda_{q1}\tilde{\xi}_q\dot{\xi}_q$$

$$\le \overline{q}_e^T\Omega_e - k_q\overline{q}_e^T\overline{q}_e - k_q K_q^{\frac{1+\Gamma_0}{2}}\left(2(1-q_{e0})\right)^{\frac{1+\Gamma_0}{2}} + k_q\delta^{1+\Gamma_0}$$

$$-\frac{2\lambda_{q2}}{(2-2k)\lambda_{q1}}\frac{1}{2}\lambda_{q1}\tilde{\xi}_q^2 - \frac{\lambda_{q2}}{2k\lambda_{q1}^l}\left(\frac{1}{2}\lambda_{q1}\tilde{\xi}_q^2\right)^l + \Delta_q$$

$$\le \overline{q}_e^T\Omega_e - c_{q1}K_q\mathbf{W}_q - c_{q2}\mathbf{W}_q^{\frac{1+\Gamma_0}{2}} + \Delta_q \tag{31}$$

where $c_{q1} = \min\left\{k_q K_q, \frac{2\lambda_{q2}}{(2-2k)\lambda_{q1}}\right\}$,

$c_{q2} = \min\left\{k_q K_q^{\frac{1+\Gamma_0}{2}}, \frac{\lambda_{q2}}{2k\lambda_{q1}^l}\right\}$,

$\Delta_q = \iota + \lambda_{q2}\xi_q^2 + \frac{\lambda_{q2}}{2k}(1-l)l^{\frac{l}{1-l}} + k_q K_q\delta^{1+\Gamma_0}$, and the parameter K_q is given by $K_q = \frac{1+q_{e0}}{2}$. The coupled term $\overline{q}_e^T\Omega_e$ will be dealt with in the next step.

Step 2: Design of a virtual controller for χ_τ.

Define the tracking error $e_\tau = \chi_\tau - \chi_{\tau d}$, where $\chi_{\tau d}$ is the virtual controller for χ_τ. The time derivative of Ω_e is

$$\dot{\Omega}_e = \dot{\omega}_x - \dot{\omega}_{xc}$$

$$= \frac{\partial\omega_x}{\partial\omega_{nb}^b}(-\mathbf{J}^{-1}\mathcal{S}(\omega_{nb}^b)\mathbf{J}\omega_{nb}^b + \mathbf{J}^{-1}\mathbf{f}(\alpha,\beta) - \mathbf{J}^{-1}\mathcal{D}\omega_{nb}^b + \mathbf{J}^{-1}\mathcal{B}\chi_\tau$$

$$+\mathbf{J}^{-1}d_\omega) - \dot{\omega}_{xc}$$

$$= \frac{\partial\omega_x}{\partial\omega_{nb}^b}(-\mathbf{J}^{-1}\mathcal{S}(\omega_{nb}^b)\mathbf{J}\omega_{nb}^b + \mathbf{J}^{-1}\mathbf{f}(\alpha,\beta) - \mathbf{J}^{-1}\mathcal{D}\omega_{nb}^b + \mathbf{J}^{-1}\mathcal{B}\chi_\tau) + f_\omega \tag{32}$$

where $f_\omega = \frac{\partial\omega_x}{\partial\omega_{nb}^b}\mathbf{J}^{-1}d_\omega - \dot{\omega}_{xc}$ is the lumped uncertainty that satisfies $\left\|f_\omega\right\| \le \zeta_\omega$ with ζ_ω being a positive constant. Consider the Lyapunov candidate $\mathbf{W}_\Omega = \frac{1}{2}\Omega_e^T\Omega_e + \frac{1}{2}\lambda_{\omega1}\tilde{\xi}_\omega^2$, where $\tilde{\xi}_\omega = \hat{\xi}_\omega - \xi_\omega$ with $\hat{\xi}_\omega$ being the estimate for ξ_ω and $\tilde{\xi}_\omega$ being the estimate error.

Design the virtual controller $\chi_{\tau d}$ as

$$\chi_{\tau d} = (\mathbf{J}^{-1}\mathcal{B})^{-1}(-(-\mathbf{J}^{-1}\mathcal{D}(\omega_{nb}^b)\mathbf{J}\omega_{nb}^b + \mathbf{J}^{-1}\mathbf{f}(\alpha,\beta)$$

$$-\mathbf{J}^{-1}\mathcal{D}\omega_{nb}^b) - \left(\frac{\partial\omega_x}{\partial\omega_{nb}^b}\right)^{-1}\left(\overline{q}_e + \psi_\Omega\right))$$

$$-\left(\frac{\partial\omega_x}{\partial\omega_{nb}^b}\right)^{-1}\left(k_\Omega\Omega_e + k_\Omega sigM(\Omega_e,\Gamma_0)\right)) \tag{33}$$

$$\psi_\Omega = \hat{\xi}_\omega\tanh\left(\frac{3k_s\hat{\xi}_\omega\Omega_e}{\iota}\right) \tag{34}$$

$$\dot{\xi}_\omega = \frac{1}{\lambda_{\omega1}}\left\|\Omega_e\right\| - \frac{\lambda_{\omega2}}{\lambda_{\omega1}}\hat{\xi}_\omega \tag{35}$$

where ψ_Ω is a robust term and $k_\Omega > 0$, $\lambda_{\omega1} > 0, \lambda_{\omega2} > 0$ are all constants to be chosen.

By implementing Lemmas 3-5, the virtual controller (33), and the inequality

$$-\lambda_{\omega2}\hat{\xi}_\omega\tilde{\xi}_\omega = -\lambda_{\omega2}\tilde{\xi}_\omega\left(\tilde{\xi}_\omega + \zeta_\omega\right)$$

$$\le -\frac{\lambda_{\omega2}}{2}\tilde{\xi}_\omega^{\,2} + \frac{\lambda_{\omega2}}{2}\zeta_\omega^2$$

$$\le -\lambda_{\omega 2}\left(\frac{1}{2k}\tilde{\xi}_{\omega}^{\ 2}+\frac{1}{2-2k}\tilde{\xi}_{\omega}^{\ 2}+\frac{1}{2k}(1-l)l^{\frac{l}{1-l}}-\frac{1}{2k}(1-l)l^{\frac{l}{1-l}}\right)$$

$$+\frac{\lambda_{\omega 2}}{2}\xi_{\omega}^{2}$$

$$\le \frac{\lambda_{\omega 2}}{2}\xi_{\omega}^{2}+\frac{1}{2k}\lambda_{\omega 2}(1-l)l^{\frac{l}{1-l}}-\frac{1}{2k}\frac{\lambda_{\omega 2}}{2^{l-1}}\frac{1}{2}\tilde{\xi}_{\omega}^{\ 2l}-\frac{\lambda_{\omega 2}}{2k-2}\tilde{\xi}_{\omega}^{2} \quad (36)$$

with $k,l=\frac{1+\Gamma_0}{2}\in(0,1)$ representing some positive constant, taking the time derivative of $\mathbf{W}_{\Omega}$ yields

$$\dot{\mathbf{W}}_{\Omega}=\Omega_e^T\left(\dot{\omega}_x-\dot{\omega}_{xc}\right)+\lambda_{\omega 1}\tilde{\xi}_{\omega}\dot{\tilde{\xi}}_{\omega}$$

$$\le \Omega_e^T\left(\frac{\partial\omega_x}{\partial\omega_{nb}^b}\mathbf{J}^{-1}\mathcal{G}e_{\tau}+\overline{q}_e-k_{\Omega}\Omega_e-k_{\Omega}sigM(\Omega_e,\Gamma_0)+f_{\Omega}-\psi_{\Omega}\right)+\left\|\Omega_e\right\|\tilde{\xi}_{\omega}$$

$$+\frac{\lambda_{\omega 2}}{2}\xi_{\omega}^{2}+\frac{1}{2k}\lambda_{\omega 2}(1-l)l^{\frac{l}{1-l}}-\frac{1}{2k}\frac{\lambda_{\omega 2}}{2^{l-1}}\frac{1}{2}\tilde{\xi}_{\omega}^{\ 2l}-\frac{\lambda_{\omega 2}}{2k-2}\tilde{\xi}_{\omega}^{2}$$

$$\le \Omega_e^T\frac{\partial\omega_x}{\partial\omega_{nb}^b}\mathbf{J}^{-1}\mathcal{G}e_{\tau}-\Omega_e^T\overline{q}_e-c_{\omega 1}\mathbf{W}_{\Omega}-c_{\omega 2}\mathbf{W}_{\Omega}^{\frac{1+\Gamma_0}{2}}+\Delta_{\omega} \quad (37)$$

where $c_{\omega 1}=\min\left\{k_{\omega},\frac{2\lambda_{\omega 2}}{(2-2k)\lambda_{\omega 1}}\right\}$, $c_{\omega 2}=\min\left\{k_{\omega},\frac{\lambda_{\omega 2}}{2k\lambda_{\omega 1}^{l}}\right\}$, and $\Delta_{\omega}=\iota+\lambda_{\omega 2}\xi_{\omega}^{2}+\frac{\lambda_{\omega 2}}{2k}(1-l)l^{\frac{l}{1-l}}+k_{\omega}\delta^{1+\Gamma_0}$.

Step 3: Design of the control law for u_{τ}.

Consider the Lyapunov candidate $\mathbf{W}_{\tau}=\frac{1}{2}e_{\tau}^Te_{\tau}$. The time derivative of $\mathbf{W}_{\tau}$ is

$$\dot{\mathbf{W}}_{\tau}=e_{\tau}^T\left(\dot{\chi}_{\tau}-\dot{\chi}_{\tau d}\right)$$

$$=e_{\tau}^T\left(\mathcal{G}_{\tau}u_{\tau}-\gamma_{\tau}\left(\chi_{\tau}-\frac{\chi_{\tau m}+\chi_{\tau M}}{2}\right)-\dot{\chi}_{\tau d}\right)$$

$$=e_{\tau}^T\left(u_{\tau}-u_{\tau}-\mathcal{G}_{\tau}u_{\tau}-\gamma_{\tau}\left(\chi_{\tau}-\frac{\chi_{\tau m}+\chi_{\tau M}}{2}\right)-\dot{\chi}_{\tau d}\right)$$

$$=e_{\tau}^T\left(u_{\tau}-\gamma_{\tau}\left(\chi_{\tau}-\frac{\chi_{\tau m}+\chi_{\tau M}}{2}\right)+f_{\tau}\right) \quad (38)$$

where $f_{\tau}=-u_{\tau}-\mathcal{G}_{\tau}u_{\tau}-\dot{\chi}_{\tau d}$ is the lumped uncertainty function which can be tackled using the following FINT observer [34].

$$\begin{cases}\dot{\hat{e}}_{\tau} &= u_{\tau}-\gamma_{\tau}\left(\chi_{\tau}-\frac{\chi_{\tau m}+\chi_{\tau M}}{2}\right)+\hat{f}_{\tau}-\gamma_0\gamma_1 sig^{\Gamma_1}(\tilde{e}_{\tau})\\ \dot{\hat{f}}_{\tau} &= -\gamma_0^2\gamma_2 sig^{\Gamma_2}(\tilde{e}_{\tau})\end{cases} \quad (39)$$

where $\hat{e}_{\tau}$ is the estimate of e_{τ} with the estimate error being defined by $\tilde{e}_{\tau}=\hat{e}_{\tau}-e_{\tau}$ and $\hat{f}_{\tau}$ is the estimate of f_{τ} with the estimate error being $\tilde{f}_{\tau}=\hat{f}_{\tau}-f_{\tau}$. It can be deduced from Lemma 6 that the estimate errors can converge to $|\tilde{f}_T|\le\Delta_{f_T}$ within a finite time, where $\Delta_{f_T}>0$ is a bounded small positive constant. Then, the control law for u_{τ} can be designed as

$$u_{\tau}=\gamma_{\tau}\left(\chi_{\tau}-\frac{\chi_{\tau m}+\chi_{\tau M}}{2}\right)-\hat{f}_{\tau}-k_{\tau}(e_{\tau}+sig^{\Gamma_0}(e_{\tau}))-\frac{\partial\omega_x}{\partial\omega_{nb}^b}\mathbf{J}^{-1}\mathcal{G}\Omega_e \quad (40)$$

where k_{τ} is positive parameter to be chosen.

Substituting (40) into (38) yields

$$\dot{\mathbf{W}}_{\tau}=e_{\tau}^T\left(\tilde{f}_{\tau}-k_{\tau}\left(e_{\tau}+sig^{\Gamma_0}(e_{\tau})\right)-\frac{\partial\omega_x}{\partial\omega_{nb}^b}\mathbf{J}^{-1}\mathcal{G}\Omega_e\right)$$

$$=e_{\tau}^T\tilde{f}_{\tau}-k_{\tau}e_{\tau}^Te_{\tau}-k_{\tau}e_{\tau}^Tsig^{\Gamma_0}(e_{\tau})-e_{\tau}^T\frac{\partial\omega_x}{\partial\omega_{nb}^b}\mathbf{J}^{-1}\mathcal{G}\Omega_e$$

$$\le -k_{\tau}\mathbf{W}_{\tau}-k_{\tau}\mathbf{W}_{\tau}^{\frac{1+\Gamma_0}{2}}-e_{\tau}^T\frac{\partial\omega_x}{\partial\omega_{nb}^b}\mathbf{J}^{-1}\mathcal{G}\Omega_e+\Delta_{\tau} \quad (41)$$

where Young's inequality is utilized and the term $\Delta_{\tau}=\sup_{t>0}\left\{\frac{1}{2k_{\tau}}\tilde{f}_{\tau}^T\tilde{f}_{\tau}\right\}$ is a positive constant.

Theorem 2 Consider the 6-DOF FW UA described by (5) with the AIS model (8) and suppose Assumptions 1, 2, and 3 are satisfied. Let the FINT attitude control law be given by (40), where the virtual controllers ω_{xc} and $\chi_{\tau d}$ are defined in (28) and (33), and the FINT disturbance observers is given by (39). Define the Lyapunov function as $\mathbf{W}_A=\mathbf{W}_q+\mathbf{W}_{\Omega}+\mathbf{W}_{\tau}$. If $\mathbf{W}_q(0)$, $\mathbf{W}_{\Omega}(0)$, and $\mathbf{W}_{\tau}(0)$ are bounded, then the attitude error q_e is FINT convergent with all considered constraint conditions strictly satisfied, indicating that the control objective can be achieved.

Proof. Using equations (31), (37), and (41), the time derivative of $\mathbf{W}_A$ can be obtained as

$$\dot{\mathbf{W}}_A\le\overline{q}_e^T\Omega_e-k_qK_q\mathbf{W}_q-k_qK_q^{\frac{1+\Gamma_0}{2}}\mathbf{W}_q^{\frac{1+\Gamma_0}{2}}+\Delta_q+\Omega_e^T\frac{\partial\omega_x}{\partial\omega_{nb}^b}\mathbf{J}^{-1}\mathcal{G}e_{\tau}-\Omega_e^T\overline{q}_e$$

$$-k_{\Omega}\mathbf{W}_{\Omega}-k_{\Omega}\mathbf{W}_{\Omega}^{\frac{1+\Gamma_0}{2}}+\Delta_{\Omega}-k_{\tau}\mathbf{W}_{\tau}-k_{\tau}\mathbf{W}_{\tau}^{\frac{1+\Gamma_0}{2}}$$

$$-e_{\tau}^T\frac{\partial\omega_x}{\partial\omega_{nb}^b}\mathbf{J}^{-1}\mathcal{G}\Omega_e+\Delta_{\tau}$$

$$\le -k_q K_q \mathbf{W}_q - k_q K_q^{\frac{1+\Gamma_0}{2}} \mathbf{W}_q^{\frac{1+\Gamma_0}{2}} - k_\Omega \mathbf{W}_\Omega$$

$$-k_\Omega \mathbf{W}_\Omega^{\frac{1+\Gamma_0}{2}} - k_\tau \mathbf{W}_\tau - k_\tau \mathbf{W}_\tau^{\frac{1+\Gamma_0}{2}} + \Delta_A$$

$$\le -c_{A1}\mathbf{W}_A - c_{A2}\mathbf{W}_A^{\frac{1+\Gamma_0}{2}} + \Delta_A \tag{42}$$

where Δ_A is a positive bounded constant defined as $\Delta_A = \Delta_q + \Delta_\Omega + \Delta_\tau$, with parameters $c_{A1} = \min\{k_q K_q, k_\Omega, k_\tau\}$ and $c_{A2} = \min\{k_q K_q^{\frac{1+\Gamma_0}{2}}, k_\Omega, k_\tau\}$. Although the parameter $K_q = 1 + q_{e0}$ implies that $K_q = 0$ might occur at certain instants, the FINT convergence of the attitude tracking error can still be guaranteed for the following reasons. Note that $q_{e0} = 1$ and $q_{e0} = -1$ are two equilibria of q_{e0}, and according to the form of the Lyapunov function $\mathbf{W}_q$, $q_{e0} = 1$ is the only stable equilibrium point. This implies that the inequality $K_q = 1 + q_{e0} > 1$ holds after a finite time interval T_q. Therefore, the conditions $c_{A1} > 0$ and $c_{A2} > 0$ can be satisfied, and thus, according to (42), the FINT convergence of $\mathbf{W}_A$ is guaranteed.

Then, based on Lemma 1, provided that $\frac{\Delta_A}{c_{A1}} \ge \left(\frac{\Delta_A}{c_{A2}}\right)^{\frac{2}{1+\Gamma_0}}$, the stacked tracking error $E_A = col(1 - q_{e0}, \Omega_e, e_\tau)$ converges within finite time $\mathfrak{T}_A$ to the set $\mathfrak{U}_m = \{\|E_A\| \mid \mathbf{W}_A \le \max\left\{\frac{\Delta_A}{c_{A1}}, \left(\frac{\Delta_A}{c_{A2}}\right)^{\frac{2}{1+\Gamma_0}}\right\}$, meaning that the FINT attitude control can be achieved. Moreover, the angular velocity of the UA follows the symmetric constraints since the variable ω_x is bounded throughout the attitude control process. The control objective can be achieved and this completes the proof.

Remark 7 Upon achieving the attitude control objective, the x-axis of the UA's ballistic coordinate system– representing its direction of motion in the inertial frame– points towards the active waypoint. Consequently, despite the amplitude and direction of the compound wind being unknown and not utilized within the designed control law, the adverse effects of wind on waypoint tracking mission can still be counteracted.

4. NUMERICAL SIMULATION

The attitude control performance for the derived control laws (23) and (40) is verified by means of numerical simulation in this section. The control objective of the FW UA is to adjust its attitude and flight direction and hence can sequentially reach a properly predefined series of waypoints.

The bounded disturbances applied to each subsystem are given by

$$d_V = 0.02 col(\sin(2t), \sin(2t), \sin(2t))\ m/s^2$$

$$d_\omega = 0.05 col(\sin(2t), \sin(2t), \sin(2t))\ Nm$$

The wind v_{wind}^n is modeled by implementing the constant wind model and the well known 1-cos(·) gust wind model, which has been widely used in literature and is formed as [43, 44]

$$\begin{cases} V_W = 0, t < t_s(j), \\ V_W = \dfrac{V_{WM}}{2}\left(1 - \cos\dfrac{\pi t}{t_e(j) - t_s(j)}\right), t \in [t_s(j), t_e(j)] \\ V_W = 0, t > t_e(j) \end{cases} \tag{43}$$

where $t_s = col(t_s(1), t_s(2), \cdots, t_s(n))$ is the moment at which the gust begins to take effect, $t_e = col(t_e(1), t_e(2), \cdots, t_e(n))$ is the time when the gust ceases to exert its effect entirely, V_{WM} is the maximum of the gust amplitude. Then, v_{wind}^n is described by $v_{wind}^n = v_{ws}^n + v_{wg}^n$, where $v_{ws}^n = col(3,0,0)$ m/s is the constant wind and $v_{wg}^n = col(0, V_M(t), 0)$ m/s is the gust wind vector. The parameters for the wind field are set to be $V_{WM} = -4$ m/s for $t \in [t_s(1), t_e(1)]$ and $V_{WM} = 4$ m/s for $t \in [t_s(2), t_e(2)]$ s, $t_s = col(5, 28)$ s, and $t_e = col(15, 38)$ s.

The parameters associated with the FW UA according to [41] is shown in Table **1**.

The parameters related to the constraints on velocities and inputs are $-\omega_m = \omega_M = col(1,1,1)$ rad/s, $\chi_{Tm} = 0.05\chi_{TM}$, $\chi_{TM} = 18$ N, $\chi_{jm} = \pi/18$ rad, $\chi_{jM} = \pi/9\ (j = a, e, r)$, and $\gamma_T = \gamma_\tau = 0.0001$. The initial conditions of the FW UA are set as $p^n(0) = col(-100, 200, 130)$ m, $q_{nb}(0) = col(\cos\left(\frac{0.85\pi}{2}\right), col(1,0,0)\sin\left(\frac{0.85\pi}{2}\right))$, $\omega_{nb}^b(0) = col(0,0,0)$ rad/s, $v_r^b(0) = col(15,0,1)$ m/s, $\chi_T(0) = 5$ N, and $\chi_\tau(0) = col(0,0,0)$ rad. The parameters of the control laws (23) and (40), as well as those of the FINT disturbance observer, are set as follows. $k_q = 0.5$, $k_\Omega = 8$, $k_\delta = 2$, $k_V = 4$, $k_T = 2$, $\delta = 0.000001$, $\Gamma_0 = 0.7$, $\Gamma_1 = 0.85$, $\Gamma_2 = 0.7$, $\gamma_0 = 15$, $\gamma_1 = 8$, and $\gamma_2 = 12$. The waypoint sequence is given as

Table 1: General Parameters of the UAV [41]

Notation	Value	Unit	Notation	Value	Unit
m	1.9	kg	ρ	1.29	kg/m^3
S_w	0.32	m^2	b	1.2	m
$\bar{c}$	0.3	m	e	0.80	/
J_{xx}	0.0894	$kg \cdot m^2$	J_{xz}	0.014	$kg \cdot m^2$
J_{yy}	0.144	$kg \cdot m^2$	J_{zz}	0.162	$kg \cdot m^2$
C_{L_0}	0.23	/	C_{L_α}	4.58	/
$C_{L_{\tau e}}$	0.13	/	C_{L_q}	7.95	/
$C_{L_{min}}$	0.23	/	C_{D_0}	0.0434	/
$C_{D_{\tau e}}$	0.0135	/	$C_{D_{\tau r}}$	0.0303	/
C_{m_0}	0.135	/	C_{m_α}	−1.5	/
$C_{m_{\tau e}}$	−1.13	/	C_{m_q}	−50.8	/
$C_{m_{\dot{\alpha}}}$	−10.4	/	C_{l_β}	−0.04	/
C_{l_p}	−0.443	/	C_{l_r}	0.499	/
$C_{l_{\tau a}}$	0.0794	/	$C_{l_{\tau r}}$	0.016	/
C_{n_β}	0.0344	/	C_{n_p}	−0.075	/
C_{n_r}	−0.411	/	$C_{n_{\tau a}}$	−0.012	/
$C_{n_{\tau r}}$	−0.0345	/	C_{Y_β}	−0.83	/
$C_{Y_{\tau r}}$	0.191	/	C_{Y_p}	0	/
C_{Y_r}	0	/			

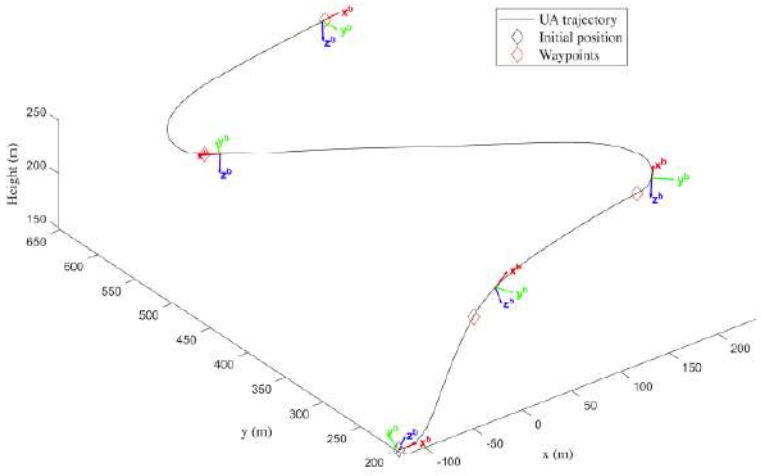

Figure 2: Trajectory of the FW UA.

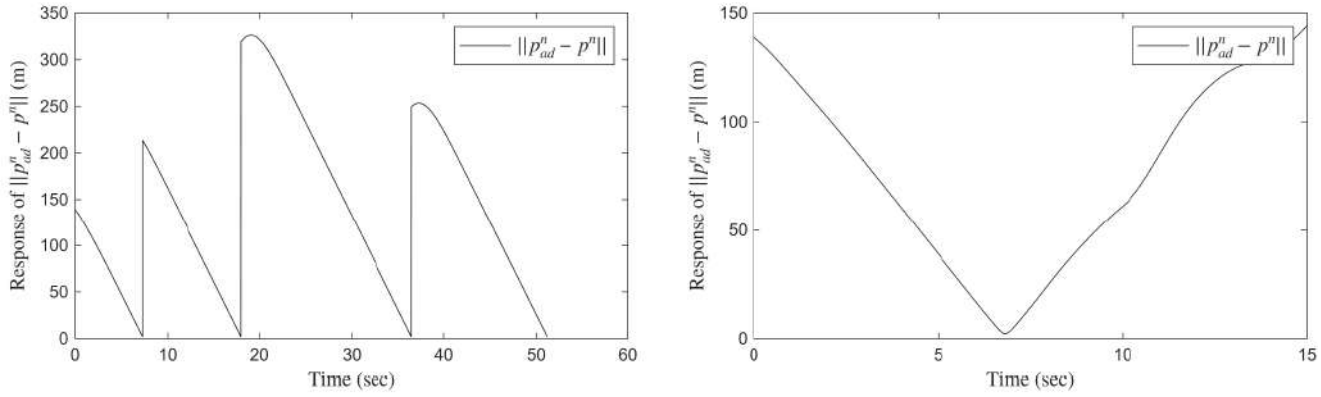

Figure 3: Distance between p_d^n and p^n when $q_e = q_{dn} \odot q_{nb}$.

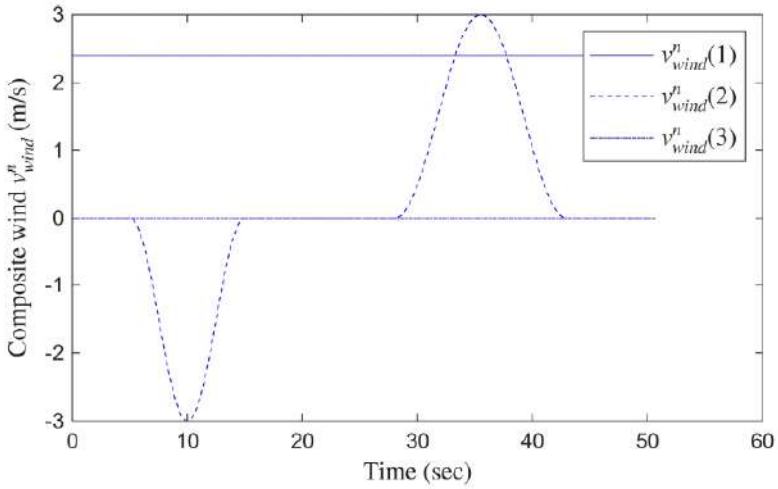

Figure 4: External unknown wind in F^n .

$$p_d^n = \begin{bmatrix} -5 & 200 & -50 & 150 \\ 250 & 300 & 500 & 650 \\ 210 & 230 & 240 & 250 \end{bmatrix} m$$

and the active waypoint switches to the next as if $\left\|p_{ad}^n - p^n\right\| \leq 2$ m, where $p_{ad}^n \in \mathbb{R}^3$ is the active waypoint.

Figures **2-4** respectively illustrate the flight trajectory of the considered aircraft, the distance between the UA and the active waypoint under the proposed control algorithm, and the curve of the external wind v_{wind}^n .

In Figure **2**, it is shown that the prescribed waypoints are reached sequentially by the FW UA. The flight direction is effectively regulated during the flight so that the second half of each flight segment toward p_{ad}^n becomes almost a straight line. This demonstrates that the attitude control objective is achieved and that the attitude error remains close to zero. Because the next waypoint can be activated only when $\left\|p_{ad}^n - p^n\right\| \leq 2\ m$ is satisfied, the proposed control law guarantees that the UA approaches p_{ad}^n with a sufficiently small distance, as is shown in Figure **3a**. The designed attitude control law can accurately align the ground velocity vector–coincident with the x -axis of F^B –toward the active waypoint. Note that $\left\|p_{ad}^n - p^n\right\|$ temporarily increases after the second waypoint is reached, since the component of the active waypoint along the x-axis of F^d is negative. Figure **3b** shows the curve of $\left\|p_d^n(1) - p^n\right\|$ when the attitude error is defined as the orientation difference between frames F^b and F^d. It is observed that $\left\|p_d^n(1) - p^n\right\|$ increases after $t > 7\ s$, indicating that the UA misses the active waypoint under external wind depicted in Figure **4**. This verifies that the influence of wind has been effectively countered by the proposed control law, confirming the robustness of the waypoint tracking policy.

Figures **5, 6** respectively show the trajectories of the airspeed V_a , the response of V_a in a wind-free environment, the thrust χ_T , and thrust under wind-free

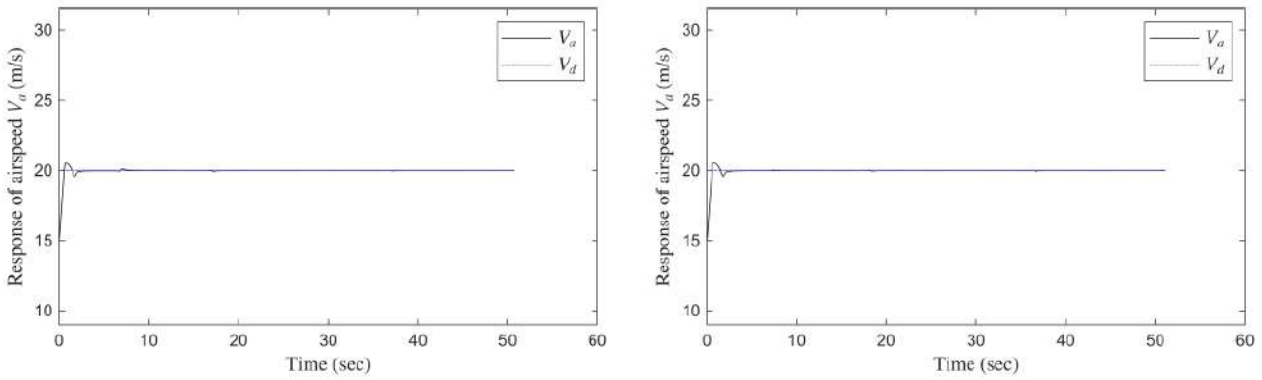

(a) V_a under influence of wind. (b) V_a under no wind condition.

Figure 5: Response of V_a under wind & wind-free environments.

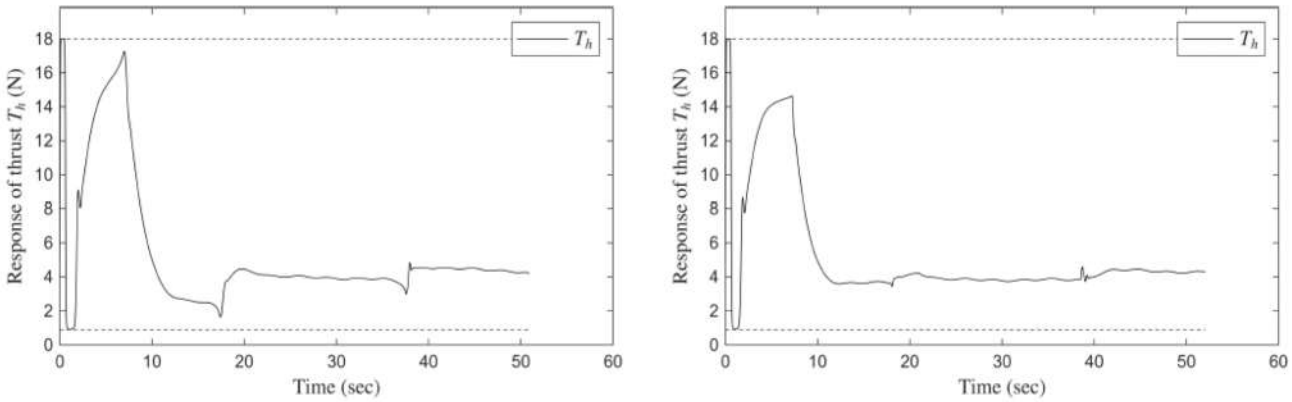

(a) Response of χ_T. (b) χ_T under wind-free condition.

Figure 6: Response of ω_{nb}^b.

condition, with the red dashed lines presented in Figure **5, 6a** indicating the respective constraints imposed on each variable. In Figure **5a**, under the action of the control algorithm for the translational subsystem, the airspeed tracks V_d, represented by the blue dotted line, within 10 s and after that the airspeed keeps tracking the command V_d even if the UA is experiencing drastic attitude adjustment when the next waypoint is about to be activated. In Figure **6a**, the thrust χ_T reaches the saturated zone in certain times. The thrust converges to constants soon after p_{ad}^n switches as the aircraft only needs to hold the airspeed while approaching p_{ad}^n. The airspeed tracking is achieved within a finite time with all the considered constraints being not violated, which verifies the effectiveness of the AIS model for translational subsystem and the designed airspeed tracking control law. Figure **6b** shows that the response of χ_T is smoother under wind-free conditions, as there is no wind to affect the magnitude of the airspeed vector. It is noteworthy that the tracking performance is not satisfactory when $t \in [0,20]$, as is shown in Figure **5a, 5b**. By comparing Figures **5a** and **5b**, we can find that the observed tracking performance reduction for $t \in [0,20]$ results from the unknown wind $\boldsymbol{v}_{wind}^n$.

As for the rotational subsystem, Figures **7-9** respectively depict the response of attitude error q_e, angular velocity ω_{nb}^b, and aerodynamic surface deflection angles χ_τ, with the red dashed lines presented in Figures **8a-9a** indicating the respective constraints imposed on each variable.

Figure **7a** shows that the attitude error increases significantly at the moments around $t = 7$ s, $t = 17$ s, and $t = 38$ s, resulting from the activation of a new waypoint. Under the action of the input χ_τ, $\boldsymbol{P}\overline{q}_e\boldsymbol{P}$ can quickly converge to near 0 each time, so as to continue to move to the new activated waypoint. It is foreseeable that the angular velocity can experience violently changing in the short period of time before and after reaching the waypoint with the applied constraint being followed, which is demonstrated by Figure **8a**. Figure **8b** shows that the angular velocity can sometimes exceed the specified limits if the velocity constraint

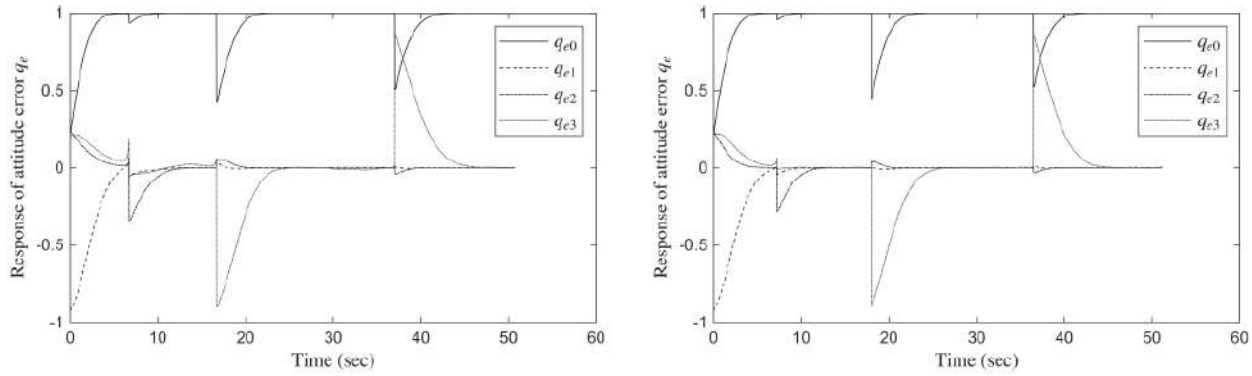

(a) q_e under external wind. (b) q_e under wind-free condition.

Figure 7: Response of q_e in wind & wind-free environments.

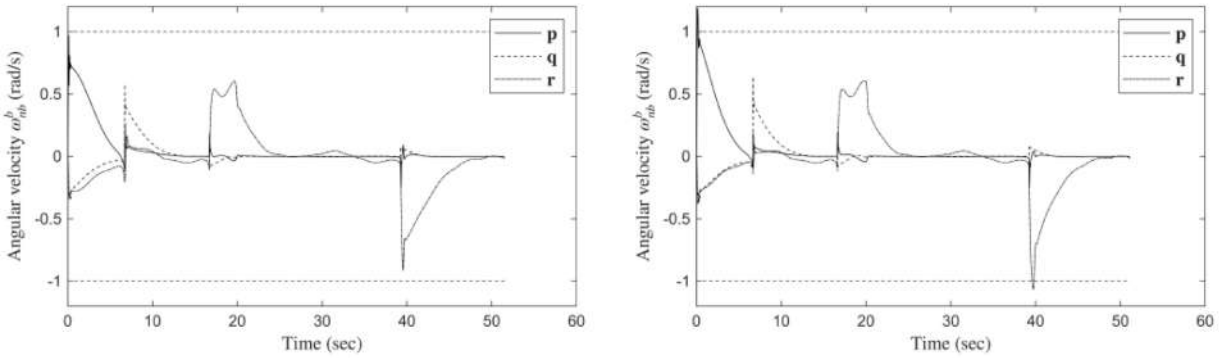

(a) Response of ω_{nb}^b. (b) ω_{nb}^b without constraint mechanism.

Figure 8: Response of ω_{nb}^b.

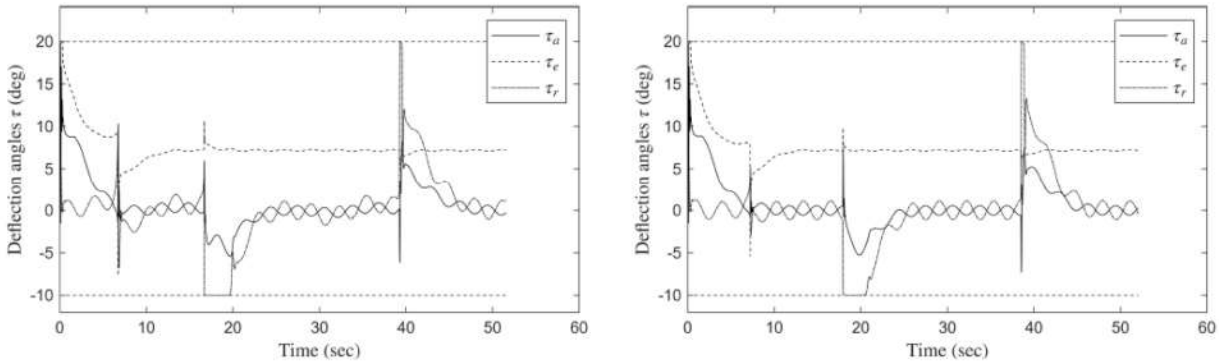

(a) Response of χ_τ. (b) Wind-free response of χ_τ.

Figure 9: Response of χ_τ.

mechanism is not applied, potentially leading to severe accidents for the FW UA. In Figure **9a**, it can be seen that χ_τ reaches the asymmetric saturation zone at certain time intervals. It can be observed from Figure **9b** that most of the deflections of the control surfaces are used to compensate for disturbances rather than for attitude tracking errors caused by wind effects. Despite that, under the influence of the devised control law (40), the input rapidly regulates the attitude of the aircraft to force the x-axis of F^B to direct toward p_{ad}^n, which is the result of $\overline{q}_e$ getting quickly stabilized.

Under the action of the proposed control law (23) and (40) for the FW UA exposed to external wind and disturbance, the FINT attitude control mission is well accomplished and the given waypoints are reached by the aircraft in turn with none of the considered constraints being violated during the flight.

5. CONCLUSION

A waypoint tracking method and a FINT attitude control algorithm for FW UA subject to angular velocity constraints, AIS, and unknown wind are proposed via the NMF and the smooth AIS model. The FINT convergence of the attitude tracking errors is ensured based on Lyapunov theory. With the developed control scheme, the transformed variables are bounded and the attitude tracking errors can reach the vicinity of the origin, meaning that the ground velocity aligns with the designated waypoint after a finite time without violating any of the considered constraints. Numerical simulation results demonstrate that the derived closed-loop system exhibits satisfactory control performance even if the UA suffers from mixed constraints, external disturbances, and unknown wind. Future work will investigate FINT attitude control for FW UA under more demanding conditions, including constraints on input rate and airspeed.

APPENDIX

6 Proof of Theorem 1

\unskip\nopunct. If $\mathcal{U}_j(t)$ remains bounded for all $t \geq 0$ and $\chi_j = \chi_{jM}$ or $\chi_j = \chi_{jm}$, then it is clear that $\mathcal{G}_j = 0$ and

$$\dot{\chi}_j = -\gamma_{uj}\left(\chi_j - \frac{\chi_{jm} + \chi_{jM}}{2}\right). \tag{44}$$

which means $\dot{\chi}_j > 0$ when $\chi_j = \chi_{jm}$ and $\dot{\chi}_j < 0$ when $\chi_j = \chi_{jM}$.

For the case $\chi_j \in (\chi_{jm}, \chi_{jM})$, define $\tilde{\chi}_j = \chi_j - \frac{\chi_{jm}+\chi_{jM}}{2}$. Consider the Lyapunov function $V_\chi = \tilde{\chi}_j^2$. Taking the time derivative of V_χ yields

$$\dot{V}_\chi = 2\tilde{\chi}_j \mathcal{G}_j u_j - 2\gamma_{uj}\tilde{\chi}_j^2. \tag{45}$$

Hence, as $\chi_j \to \chi_{jM0}$ or $\chi_j \to \chi_{jm0}$ with $\chi_{jM0} \in (\chi_{jM}^-, \chi_{jM})$ and $\chi_{jm0} \in (\chi_{jm}, \chi_{jm}^+)$, $\mathcal{G}_j \to 0$, which ensures that $\dot{V}_\chi < 0$. This indicates that χ_j converges towards the equilibrium $\chi_j = \frac{\chi_{jM}+\chi_{jm}}{2} \in (\chi_{jm}, \chi_{jM})$. Then it follows that, if $u_j(t)$ is bounded for all $t \geq 0$, χ_j remains within the interval (χ_{jm}, χ_{jM}) and $\mathcal{G}_j > 0$.

This completes the proof of Theorem 1.

REFERENCES

[1] Kim T, Qiao D. Energy-efficient data collection for IoT networks via cooperative multi-hop UAV networks. IEEE Trans Veh Technol 2020; 69(11): 13796-811. https://doi.org/10.1109/TVT.2020.3027920

[2] Lin X, Niu Y, Yu X, Fan Z, Zhuang J, Zou AM. Paying more attention on backgrounds: Background-centric attention for UAV detection. Neural Networks 2025; 185: 107182. https://doi.org/10.1016/j.neunet.2025.107182

[3] Oh H, Kim S, Shin HS, Tsourdos A, White B. Coordinated standoff tracking of moving target groups using multiple UAVs. IEEE Trans Aerosp Electron Syst 2015; 51(2): 1501-14. https://doi.org/10.1109/TAES.2015.140044

[4] Chen YJ, Chang DK, Zhang C. Autonomous tracking using a swarm of UAVs: A constrained multi-agent reinforcement learning approach. IEEE Trans Veh Technol 2020; 69(11): 13702-17. https://doi.org/10.1109/TVT.2020.3023733

[5] Motamedi A, Mortazavi M, Sabzehparvar M, Duchon F. Minimum time search using ant colony optimization for multiple fixed-wing UAVs in dynamic environments. Appl Soft Comput 2024; 165: 112025. https://doi.org/10.1016/j.asoc.2024.112025

[6] Fredriksen E, Pettersen KY. Global κ-exponential way-point maneuvering of ships: Theory and experiments. Automatica 2006; 42(4): 677-87. https://doi.org/10.1016/j.automatica.2005.12.020

[7] Oland E, Schlanbusch R, Kristiansen R. Underactuated waypoint tracking of a fixed-wing UAV. IFAC Proc Vol 2013; 46(30): 126-33. https://doi.org/10.3182/20131120-3-FR-4045.00007

[8] Rout R, Subudhi B. Narmax self-tuning controller for line-of-sight-based waypoint tracking for an autonomous underwater vehicle. IEEE Trans Control Syst Technol 2017; 25(4): 1529-36. https://doi.org/10.1109/TCST.2016.2613969

[9] Jing A, Gao J, Min B, Wang J, Chen Y, Pan G, et al. Energy-efficient waypoint tracking for underwater gliders: theory and experimental results. IEEE Trans Cybern 2025; 55(9): 4064-77. https://doi.org/10.1109/TCYB.2025.3578122

[10] Muralidharan V, Mahindrakar AD. Position stabilization and waypoint tracking control of mobile inverted pendulum robot. IEEE Trans Control Syst Technol 2014; 22(6): 2360-7. https://doi.org/10.1109/TCST.2014.2300171

[11] Wang J, Zhao L, Liu F, Xia K. Online robot navigation using discrete waypoints via time-varying guidance vector fields. IEEE Trans Ind Electron 2025; 72(3): 2987-96. https://doi.org/10.1109/TIE.2024.3436533

[12] Duda H. Effects of rate limiting elements in flight control systems - A new PIO-criterion. In: Guidance, Navigation, and Control Conference. American Institute of Aeronautics and Astronautics; 1995. https://doi.org/10.2514/6.1995-3204

[13] Klyde DH, Mitchell DG. Investigating the role of rate limiting in pilotinduced oscillations. J Guid Control Dyn 2004; 27(5): 804-13. https://doi.org/10.2514/1.3215

[14] Lv M, Li Y, Wan L, Dai J, Chang J. Fast nonsingular fixed-time fuzzy fault-tolerant control for HFVs with guaranteed time-varying flight state constraints. IEEE Trans Fuzzy Syst 2022; 30(11): 4555-67. https://doi.org/10.1109/TFUZZ.2022.3157393

[15] Kim Sh, Kim M, Kim Y. Fault-tolerant adaptive control for trajectory tracking of a quadrotor considering state constraints and input saturation. IEEE Trans Aerosp Electron Syst 2024; 60(3): 3148-59.

https://doi.org/10.1109/TAES.2024.3360021

[16] Lv M, Ahn CK, Zhang B, Fu A. Fixed-time antisaturation cooperative control for networked fixed-wing unmanned aerial vehicles considering actuator failures. IEEE Trans Aerosp Electron Syst 2023; 59(6): 8812-25. https://doi.org/10.1109/TAES.2023.3311420

[17] Duan H, Yuan Y, Zeng Z. Distributed cooperative control of multiple UAVs in the presence of actuator faults and input constraints. IEEE Trans Circuits Syst II 2022; 69(11): 4463-7. https://doi.org/10.1109/TCSII.2022.3181442

[18] Zhang B, Sun X, Lv M, Liu S, Li L. Distributed adaptive fixed-time fault-tolerant control for multiple 6-DOF UAVs with full-state constraints guarantee. IEEE Syst J 2022; 16(3): 4792-803. https://doi.org/10.1109/JSYST.2021.3128973

[19] Yang XR, Lin X, Yang Y, Zou AM. Finite-time attitude tracking control of rigid spacecraft with multiple constraints. IEEE Trans Aerosp Electron Syst 2024; 60(3): 3688-97. https://doi.org/10.1109/TAES.2024.3356983

[20] Zou AM, Kumar KD. Finite-time attitude control for rigid spacecraft subject to actuator saturation. Nonlinear Dynam 2019; 96(2): 1017-35. https://doi.org/10.1007/s11071-019-04836-7

[21] Ji J, Zhang Z, Zuo Z, Wang Y. Event-triggered global consensus of second-order multi-agent systems with asymmetric input saturation. Neurocomputing 2024; 574: 127287. https://doi.org/10.1016/j.neucom.2024.127287

[22] Wang M, Huang L, Yang C. NN-based adaptive tracking control of discrete-time nonlinear systems with actuator saturation and event-triggering protocol. IEEE Trans Syst, Man, Cybern, Syst 2021; 51(12): 7613-21. https://doi.org/10.1109/TSMC.2020.2981954

[23] Wang K, Wen SX, Gao YF, Zhang X, Sun XM. Switching anti-windup synthesis for linear systems subject to asymmetric input magnitude and rate saturation: Application to aircraft engines. IEEE Trans Aerosp Electron Syst 2024; 60(2): 1924-36. https://doi.org/10.1109/TAES.2023.3346803

[24] Arya SR, Rao S, Dattaguru B. Effect of asymmetric control constraints on fixed-wing UAV trajectories. IEEE Trans Aerosp Electron Syst 2019; 55(3): 1407-19. https://doi.org/10.1109/TAES.2018.2871435

[25] Zhou Y, Dong W, Liu Z, Lv M, Zhang W, Chen Y. IBLF-based fixedtime fault-tolerant control for fixed-wing UAV with guaranteed timevarying state constraints. IEEE Trans Veh Technol 2023; 72(4): 4252-66. https://doi.org/10.1109/TVT.2022.3223121

[26] An B, Fan H, Wang B, Liu L, Wang Y. Velocity-constrained distributed formation tracking of fixed-wing UAVs with multiple leaders. Aerosp Sci Technol 2024; 154: 109514. https://doi.org/10.1016/j.ast.2024.109514

[27] Jiao D, Wang Y, Chen Y, Lu W, Zou AM. Finite-time attitude control for fixed-wing UAVs with full-state constraints and input saturation. J Franklin Inst 2025; 342(4): 107522. https://doi.org/10.1016/j.jfranklin.2025.107522

[28] Lai B, Tang Y, Wang Y, Jiao D, Zou AM. Finite-time attitude tracking control for rigid spacecraft subject to angular velocity constraints and input magnitude and rate saturation. Aerosp Sci Technol 2025; 160: 110084. https://doi.org/10.1016/j.ast.2025.110084

[29] Bauersfeld L, Spannagl L, Ducard G, Onder C. MPC flight control for a tilt-rotor VTOL aircraft. IEEE Trans Aerosp Electron Syst 2021; 57(4): 2395-409. https://doi.org/10.1109/TAES.2021.3061819

[30] Manzoor T, Xia Y, Zhai DH, Ma D. Trajectory tracking control of a VTOL unmanned aerial vehicle using offset-free tracking MPC. Chinese J Aeronaut 2020; 33(7): 2024-42. https://doi.org/10.1016/j.cja.2020.03.003

[31] Li X, Zhang H, Fan W, Wang C, Ma P. Finite-time control for quadrotor based on composite barrier Lyapunov function with system state constraints and actuator faults. Aerosp Sci Technol 2021; 119: 107063. https://doi.org/10.1016/j.ast.2021.107063

[32] Liu Y, Zhang H, Sun J,Wang Y. Adaptive fuzzy containment control for multiagent systems with state constraints using unified transformation functions. IEEE Trans Fuzzy Syst 2022; 30(1): 162-74. https://doi.org/10.1109/TFUZZ.2020.3033376

[33] Yu L, He G,Wang X, Zhao S. Robust Fixed-Time Sliding Mode Attitude Control of Tilt Trirotor UAV in Helicopter Mode. IEEE Trans Ind Electron 2022; 69(10): 10322-32. https://doi.org/10.1109/TIE.2021.3118556

[34] Zou AM, de Ruiter AHJ, Kumar KD. Disturbance observer-based attitude control for spacecraft with input MRS. IEEE Trans Aerosp Electron Syst 2019; 55(1): 384-96. https://doi.org/10.1109/TAES.2018.2852369

[35] Yu S, Yu X, Shirinzadeh B, Man Z. Continuous finite-time control for robotic manipulators with terminal sliding mode. Automatica 2005; 41(11): 1957-64. https://doi.org/10.1016/j.automatica.2005.07.001

[36] Bhat SP, Bernstein DS. Continuous finite-time stabilization of the translational and rotational double integrators. IEEE Trans Autom Control 1998; 43(5): 678-82. https://doi.org/10.1109/9.668834

[37] Hong Y, Hu J, Gao L. Tracking control for multi-agent consensus with an active leader and variable topology. Automatica 2006; 42(7): 1177-82. https://doi.org/10.1016/j.automatica.2006.02.013

[38] Hardy GH, Littlewood JE, PoÅLlya G. Inequalities. Cambridge, U.K.: Cambridge University Press; 2001.

[39] Polycarpou MM, Ioannou PA. A robust adaptive nonlinear control design. Automatica 1996; 32(3): 423-7. https://doi.org/10.1016/0005-1098(95)00147-6

[40] Qian C, Lin W. Non-Lipschitz continuous stabilizers for nonlinear systems with uncontrollable unstable linearization. Syst Control Lett 2001; 42(3): 185-200. https://doi.org/10.1016/S0167-6911(00)00089-X

[41] Paw YC. Synthesis and validation of flight control for UAV [Ph.D. dissertation]. Minneapolis, MN, USA: University of Minnesota; 2009.

[42] Raol JR, Singh J. Flight Mechanics Modeling and Analysis. 2nd ed. Boca Raton, FL: CRC PRESS; 2023. https://doi.org/10.1201/9781003293514

[43] Lungu M. Auto-landing of fixed wing unmanned aerial vehicles using the backstepping control. ISA Trans 2019; 95: 194-210. https://doi.org/10.1016/j.isatra.2019.05.019

[44] Xing Z, Zhang Y, Su CY. Active wind rejection control for a quadrotor UAV against unknown winds. IEEE Trans Aerosp Electron Syst 2023; 59(6): 8956-68. https://doi.org/10.1109/TAES.2023.3315254